BRNO UNIVERSITY OF TECHNOLOGY
VYSOKÉ UČENÍ TECHNICKÉ V BRNĚ

FACULTY OF CHEMISTRY
FAKULTA CHEMICKÁ

INSTITUTE OF MATERIALS SCIENCE
ÚSTAV CHEMIE MATERIÁLŮ

MICROFIBERS BASED ON POLYHYDROXY-BUTYRATE FOR MEDICAL APPLICATIONS

MIKROVLÁKNA NA BÁZI POLYHYDROXYBUTYRÁTU PRO MEDICÍNSKÉ APLIKACE

MASTER'S THESIS
DIPLOMOVÁ PRÁCE

AUTHOR **Bc. ZUZANA GREGUŠKOVÁ**
AUTOR PRÁCE

SUPERVISOR **Mgr. RADEK PŘIKRYL, Ph.D.**
VEDOUCÍ PRÁCE

BRNO 2021

BRNO UNIVERSITY OF TECHNOLOGY
FACULTY OF CHEMISTRY

Specification Master's Thesis

Project no.:	FCH-DIP1601/2020	Academic year:	2020/21
Department:	Institute of Materials Science		
Student:	**Bc. Zuzana Gregušková**		
Study programme:	Chemistry, Technology and Properties of Materials		
Study field:	Chemistry, Technology and Properties of Materials		
Head of thesis:	**Mgr. Radek Přikryl, Ph.D.**		

Title of Master's Thesis:

Microfibers based on polyhydroxybutyrate for medical applications

Master's Thesis:

Carry out a search on the topic of biopolymer microfibers for medical applications, get acquainted with the technology of centrifugal spinning. Prepare polymer solutions or mixtures thereof and produce microfibers. Optimize process parameters (viscosity, speed, mixture composition, etc.) with regard to the resulting properties of the fibers (fiber diameter distribution, mechanical properties, etc.) and, if necessary, perform or ensure selected biocompatibility tests.

Deadline for Master's Thesis delivery: 28.5.2021:

Master's Thesis should be submitted to the institute's secretariat in a number of copies as set by the dean This specification is part of Master's Thesis

Bc. Zuzana Gregušková Student	Mgr. Radek Přikryl, Ph.D. Head of thesis	doc. Ing. František Šoukal, Ph.D. Head of department

In Brno dated 1.2.2021

prof. Ing. Martin Weiter, Ph.D.
Dean

Abstract

Master's thesis targets microfibers based on biopolymer poly(3-hydroxybutyrate) and their use in medical applications. The theoretical part deals with a study of the microfibers creation process using the technology of centrifugal spinning, its kinetics and factors influencing the creation and properties of prepared microfibres. Subsequently, the theoretical part orientates on a short overview of biopolymers used in the technology, characterization of material poly(3-hydroxybutyrate). It also presents a proposal of a potential target application of the microfibres. The experimental part concentrates on microfibers preparation from the mentioned poly(3-hydroxybutyrate). Several parameters leading to better spinnability of the material are tracked and optimized. The practical part is extended by modifying the polymer solution by adding other biopolymers and plasticizers and producing microfibres from the polymer mixture thus treated. Attention is also paid to the optimization of process parameters. Moreover, the prepared microfibres are analyzed and characterized by several methods and compared to develop a suitable alternative to currently used substrates for cell growth in 3D.

Abstrakt

Diplomová práca je zameraná na mikrovlákna na báze biopolyméru poly(3-hydroxybutyrátu) a ich využitie v medicínskych aplikáciách. Teoretická časť práce sa zaoberá štúdiom procesu tvorby vláken pomocou technológie odstredivého zvlákňovania, jeho kinetikou a faktormi ovplyvňujúcimi vznik a vlastnosti vláken. Teoretická časť sa následne orientuje na krátky prehľad biopolymérov používaných v tejto technológii, charakteristiku materiálu poly(3-hydroxybutyrátu) a taktiež prezentuje návrh potenciálnej cieľovej aplikácie daných mikrovláken. Praktická časť sa koncentruje sa prípravu mikrovláken zo spomínaného poly(3-hydroxybutyrátu). Sledované a optimalizované sú viaceré parametre vedúce k lepšej zvlákniteľnosti materiálu. Praktická časť je rozšírená o modifikáciu polymérneho roztoku prídavkom iných biopolymérov a zmäkčovadiel a prípravu mikrovláken z takto modifikovanej polymérnej zmesi. Pozornosť je venovaná taktiež optimalizácii procesných parametrov. Pripravené mikrovlákna sú následne analyzované a charakterizované viacerými metódami a vzájomne porovnávané s cieľom vyvinúť alternatívu k súčasne používaným substrátom pre rast buniek v 3D.

Keywords

microfibers, centrifugal spinning, poly(3-hydroxybutyrate), cell proliferation

Klíčová slova

mikrovlákna, odstredivé zvlákňovanie, poly(3-hydroxybutyrát), proliferácia buniek

GREGUŠKOVÁ, Zuzana. *Microfibers based on polyhydroxybutyrate for medical applications*. Brno, 2021. Master's thesis. Brno University of Technology, Faculty of Chemistry. Supervisor Mgr. Radek Přikryl, Ph.D.

Declaration

I declare that I have prepared the master's thesis independently and have cited all the literary sources used correctly and completely. The master's thesis is the property of the Faculty of Chemistry, Brno University of Technology. It can be used for commercial purposes only with the consent of the thesis supervisor and the dean of the Faculty of Chemistry of the Brno University of Technology.

.....
Zuzana Gregušková
May 27, 2021

Acknowledgements

Sincerely, I would like to thank my supervisor, Mgr. Radek Přikryl, Ph.D., for the time he devoted to this master's thesis to be created in the form in which I submit it for defence. Without his support, extraordinary human approach and patience, this work could never have come into being. My thanks also go to Ing. Jana Růžičková, Ph.D. for her remarkable commitment and help in preparing samples for this thesis. Finally, I would like to express my gratitude for the expert advice from my consultant doc. Ing. Lucy Vojtová, Ph.D. and also from the scientist of Department of Tissue Engineering Mgr. Michala Rampichová, Ph.D. for willingness to perform biological tests necessary for the elaboration of this work. Finally, I would like to thank Bc. Josef Kolář from the bottom of my heart for his constant help and motivation during the writing of this work.

Contents

1 Introduction

The centrifugal spinning technology and fibres produced this way gained attention several years ago due to their high production rate and easy preparation of fibres via modifying major process parameters (concentration of the polymer, rotational speed of the spinneret, selection of solvent). Fibres prepared in the form of the fibrous mat can be used for tissue engineering applications [1].

As the skin undergoes many injuries through life, there is a strong need in reconstructive medicine to find new approaches and materials for wound dressing and effective skin regeneration. The intended material should fulfil several properties, including nontoxicity, biocompatibility, antisepsis, and mechanical strength [2]. The ideal wound healing material must also provide sufficient elasticity to fit the wound shape, maintain a moist environment and preserve gaseous exchange [3].

Polyhydroxyalkanoates as biocompatible polymers play a strategic role in this field. Several scientific studies report that the proliferation of diverse cells is facilitated using scaffolds prepared from polyhydroxyalkanoates. There is also evidence about the better growth of fibroblasts and keratinocytes on polyhydroxyalkanoates based scaffolds [3].

The theoretical part of this work will concentrate on microfibers and their formation using centrifugal spinning technology. The principle of forming the microfibres and kinetics of the process will be described in more detail, followed by a chapter on the parameters influencing the centrifugal spinning process. The potential use of this technology in medicine will also be mentioned. In the second part of the theoretical part, attention will be focused on the characteristics of biopolymers that can be spun by this technology and what properties of the resulting fibres can be obtained.

In the experimental part, the dosing system of the centrifugal spinning device was modified. Optimisation of process parameters was performed on the initially prepared P(3-hydroxybutyrate) solutions to find the spinning limits of individual solutions. Different types of fibres were prepared by variation with the chemical composition of the solution and process parameters, which were subsequently characterised by selected methods and techniques focusing on the reproducibility of their production, morphology, mechanical and biological properties.

2 Theoretical part

The theoretical part of the work is divided into two parts. The first of them deals with the description of the technology used for the preparation of fibres. In the second part, biopolymers suitable for the preparation of fibres by a given technology and their application in medicine are further characterised.

2.1 Microscopic fibres

Since the outcome of the master´s thesis is microfibrous substrates, the following chapter and other chapters presented in the theoretical part of the work will be devoted exclusively to microfibers.

2.1.1 Characterisation of microfiber properties

The microfiber is, in general, defined as any fibre with a diameter of fewer than 10 micrometres [4]. However, this definition does not state the exact size limit, type or shape of the fibres and the length to diameter ratio that meets the definition of microfibres. In order to achieve consensus that will contribute to the research of microfibres, Liu et al. proposed a general definition based on several partial definitions. The definition is worded: 'Microfibers are any natural or artificial fibrous materials of threadlike structure with a diameter less than 50 µm, length ranging from 1 µm to 5 mm, and length to diameter ratio greater than 100' [5].

Microfibres excel due to their high surface area caused by their porous structure, low diameter and flexibility. Because of their attractive properties, microfibres can be applied in various application fields. The fibrillar structure of microfibres could also mimic the skin´s extracellular matrix (ECM). [1, 6, 7].

An extensive molecule network looking like a lattice describes the structure of ECM. It is composed of collagen, glycosaminoglycans, proteoglycans and glycoproteins, but its exact composition depends on the species. ECM is a non-cellular structure that consists of several types of fibrous proteins, including collagen, elastin or fibronectin [8, 9]. The schematic structure of connective tissue with the extracellular matrix is presented in the figure 2.1.

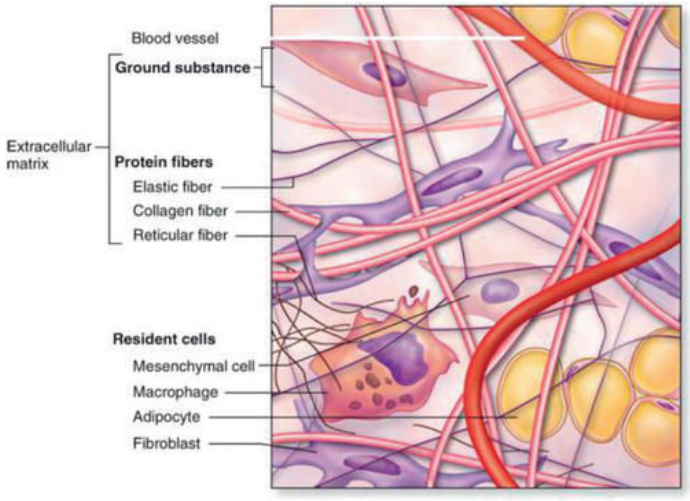

Figure 2.1: Schematic composition of connective tissue with extracellular matrix composed of several types of fibres (taken from [8])

2.1.2 Production of microfibres

In the following chapter, several microfiber production techniques will be briefly described.

Melt-blown and spun-bond process

Melt-blown technology represents a one-step process that directly converts a polymer into continuous low diameter fibres. The principle of the method is an extrusion of polymer melt with low viscosity through a single row of very fine holes. The holes are located close together in the order of 1,000–4,000 holes per m. The hot air flows from both sides at the output of the row. In this way, the hot air keeps the polymer in a molten state. The airstream develops a flutter, the fibres flap quickly back and forth, and they are cooled down by surrounding air. Finally, the fibres are situated on a random laid nonwoven fabric. Fibres produced through the melt-blow process achieve diameter in the range 1–5 µm. Still, the final fibre diameter distribution could be broader. The technology works as a large-scale commercial process that can produce fabrics on large rolls directly. Usually, the melt-blown webs are used as filtration substrates, barrier fabrics or oil absorption mats [10, 11, 12].

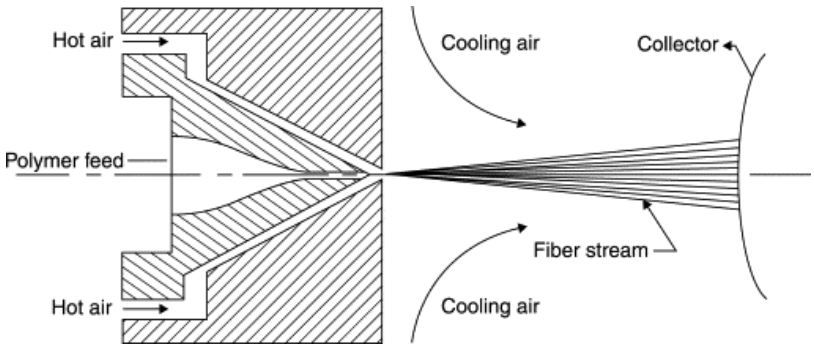

Figure 2.2: Schematic configuration of melt-blown technology (taken from [12])

The process is similar to spun-bond technology. The difference lies in the die assembly, especially in the direction in which the air flows. In the melt-blown process, the air flows parallel to the fibres emerging from the die. However, spun-bond technology is designed with air crossing the flow of emerging fibres. The result is that the melt-blown process produces finer fibres than spun-bond technology as they are not modified by hot air. The manufactured melt-blown webs are softer, bulkier and weaker. In comparison with spun-bond webs, their pore size is smaller [10].

Electrospinning

Electrostatic spinning or shortly electrospinning defines a technique for the production of continuous submicron or nanometer fibres. The method is based on the usage of the electric field, which is applied to polymer solution stored in a positively charged capillary. The electric field can convert a polymer solution drop into a so-called fine liquid jet, which produces thin fibres. The prepared fibres are placed on a grounded collector. The configuration of the electrospinning technology is shown in the figure 2.3 [13, 14, 15, 16].

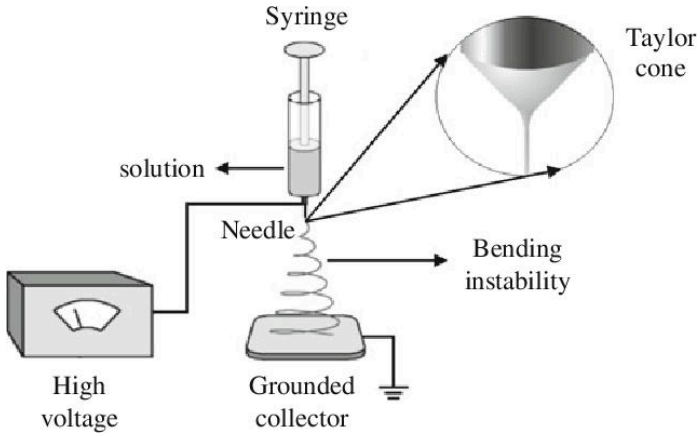

Figure 2.3: Schematic configuration of electrospinning technology (taken and slightly modified from [17])

The fibres could be fabricated using electrospinning not only from polymers but also metals, ceramics and composites. The electrospinning process is affected by several factors, including polymer concentration, solution viscosity and flow rate, electric field intensity, work distance and air humidity. The process must run in a closed chamber under controlled conditions of temperature and relative humidity. The closed chamber also decreases the danger for the user while working with high-voltage and volatile solvents [13, 18].

2.2 Centrifugal spinning

Centrifugal spinning technology, also called rotary spinning or rotational jet spinning in some publications, describes a method originally developed in 1924 by Hooper. The aim was to produce artificial silk threads from viscose or equivalent substances, and this was achieved by applying centrifugal forces to the viscous material [19]. Modern devices based on this principle provide the possibility of producing fibres with a diameter below 500 nm [20].

2.2.1 The principle of the method

The centrifugally spinning machine is composed of several parts, which are presented in figure 2.4. In the centre is located a spinneret that acts as a reservoir for polymer solution as well. The spinneret has a T-shape with one hole on the top of the spinneret to inject the polymer solution and two outputs on opposite sides. Around the spinneret, there are many collectors, which function like a catcher for produced fibres [21].

The centrifugal spinning process consists of three stages, which could be briefly described as follows. At the beginning of the spinning process, the polymer solution must be introduced into the rotary spinneret (the first stage). During rotation after overcoming the surface tension inside the spinneret, the polymer solution is ejected from the spinneret in the form of jets (the second stage). The solvent is evaporating during the creation of jets. As a result, formed dried nanofibres are deposited on the collectors. The process of drying is also connected with stretching the fibres [21, 22].

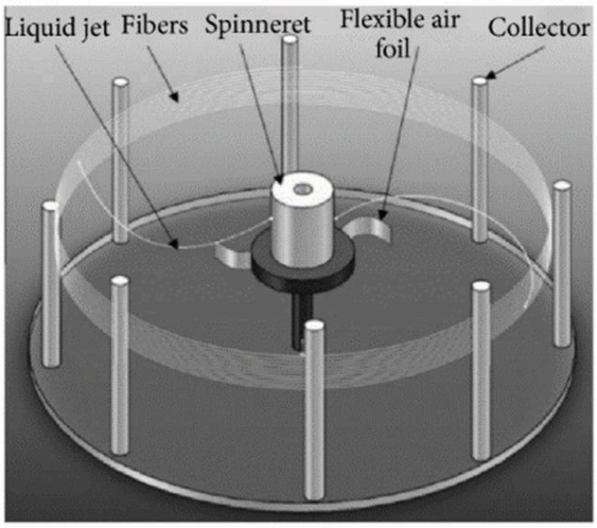

Figure 2.4: Schematic configuration of centrifugal spinning (taken from [21])

To successfully prepare fibres, it is essential to understand the three stages of fibres formation by centrifugal spinning technology. The first stage starts by injecting the material into the spinneret. While material rotating in the spinneret, it is forced by many forces, including friction, gravity, surface tension and centrifugal force. However, surface tension and centrifugal force have the most significant influence on the material. The end of the first stage comes when the solution droplet originating from the orifice reaches the orifice's lower edge.

The second phase begins when the surface tension inside the orifice is overcome by centrifugal force. The centrifugal force at which jets form has a specific value related to a particular process. It is also possible to calculate critical angular velocities when jets begin to form.

During the third phase, the solvent evaporates from the formed jets. At the same time, the individual jets expand with inertial force. This process reduces the diameter of the fibres so that the technology can also serve to form nanofibers.

Like many other technologies, centrifugal spinning technology depends on many parameters that directly or indirectly affect the formation and properties of the prepared fibre. Among the given parameters are:

- surface tension,
- the viscosity of the solution,
- speed of the spinneret,
- a distance of the collector,
- evaporation rate of the solvent [22].

Selected parameters and their influence will be the subject of this work.

2.2.2 Advantages over electrospinning technology

The electrospinning process as a technology suitable for producing microfibers, which are often used in the medical industry (such as in scaffolds, drug delivery systems, wound dressings etc.), was briefly described in the chapter devoted to the production of microfibers. Since both electrospinning and centrifugal spinning technologies produce fibres suitable for the same use, it is appropriate to compare them with each other [16].

A big advantage of centrifugal spinning technology compared with electrospinning is that it does not need high voltage for running the process. Electrical energy is used for rotating the spinneret. If the rotational speed is increased, the production efficiency is improved. In contrast, the productivity of electrospinning is low. One of the relevant disadvantages of electrospinning is also its dependence on the environment. Only a slight change in humidity influence the production of fibres and their quality. Moreover, the production of fibres could be carried out only from polymer solutions with low concentrations. If the volume of used solvents should be decreased, the centrifugal spinning technology can fulfil this ambition [1, 21]. However, based on the literature review, the concentration of P3HB solutions for electrospinning varies from 3 to 10%. Therefore this parameter is not relevant for the comparison [23, 24].

2.3 Biopolymers suitable for centrifugal spinning technology

Various natural or synthetic polymers have been tested and spun using centrifugal spinning technology. Given that the work focuses on the preparation of fibrous substrates for medicine, the following chapter will briefly present the biopolymers used in this work.

2.3.1 Poly(3-hydroxybutyrate)

Poly (3-hydroxybutyrate) (P3HB) is the best known and first identified member of the group of polyhydroxyalkanoates (PHAs), which consist of hydroxycarboxylic acid molecules. PHA biopolymers, such as natural polyesters, are produced during fermentation by various types

of bacteria that include a specific class of enzymes called PHA synthases. The fermentation process is carried out under nutrient-restricting conditions with an excess of carbon. Together with the bacterial strain and the carbon source, growth conditions are the main factors influencing the resulting molecular weight of PHA [25, 26, 27, 28].

Chemical properties

P3HB, as a polyester synthetized by bacteria, is produced in only one optically active form, which leads to reaching a high percentage of P3HB crystallinity. The crystallinity of P3HB can achieve the value above 60%. The structure of P3HB with a chiral centre is presented in figure 2.5 [29, 30].

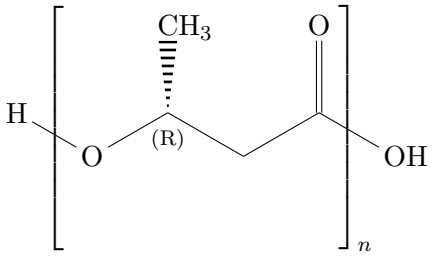

Figure 2.5: Poly(3-hydroxybutyrate)

The application of P3HB in the medical industry is discussed due to its attractive properties, such as biodegradability within the body or the fact that it is a polyester like polyglycolide. The similarity to polyglycolide is enhanced by the fact that P3HB, the same as polyglycolide, degrades by hydrolysis. Degradation of P3HB results in the formation of hydroxybutyric acid, which, like glycolic acid and lactic acid, is a naturally occurring metabolite in the body [29].

Physical and mechanical properties

The mechanical properties of P3HB are similar to PET. The glass transition temperature of P3HB reaches approximately 10 °C. In comparison with PET, there is a slight difference in terms of hydrophobicity. P3HB exhibits less hydrophobic behaviour, which results in its higher water absorption. Except for comparison with PET, the selective properties of P3HB are very similar to polypropylene (PP). Water contact angle is published in range of 70–75°. An overview of selected properties and their comparison between P3HB and PP is presented in table 2.1 [26, 29].

Table 2.1: Comparison of selected properties of P3HB and PP ([26])

Particular property	**P3HB**	**PP**
Melting point	171–182	171–186
Crystallinity	65–80	65–70
Density	1.23–1.25	0.905–0.940
Molecular weight	1–8	2.2–7.0
UV light resilience	good	weak
Solvents resilience	weak	good
Biodegradability	good	–

P3HB is a naturally thermoplastic polymer with a melting point around 180 °C which means that it could be processed as a traditional thermoplastic.A limitation is the relatively narrow processing window due to its thermal degradation. The temperatures between -30 and 120 °C indicate a range in which P3HB can be used, provided that the original shape is maintained. However, a relatively big disadvantage is the stiffness and brittleness of P3HB. The possible application options are therefore limited [31].

Application of PHAs in skin tissue engineering

The main advantages of using PHAs in skin tissue engineering are their biocompatibility and non-toxic degradation product – 3-hydroxybutyric acid naturally occurred in blood. Biocompatibility of several PHAs prepared in the form of scaffolds was studied using various skin types, including keratinocyte cell line (HaCaT) and fibroblasts. The several PHAs that undergone the investigation were: P(3HB-co-3HV-co-HHx), P(3HB), P(3HB-co-3HV), P(3HB-co-3HHx), P(3HB-co-4HHx), P(3HB-co-3HV-co-3HHx), P(4HB). Sankar et al. concentrated on the scaffold preparation from PHAs and their application in wound healing. It was investigated that the porous structure of scaffolds (which on their scaffolds reached 67 %) is an advantage for adhesion and proliferation of Human Dermal Fibroblast cells [32].

Furthermore, in combination with a hydrogel, the scaffolds indicate controlled swelling and biodegradation appropriate for wound healing application. Based on Veleirinho et al. study results, the increased content of PHAs (specifically P(3HB-co3HV)) used in the nanofibrous scaffold blend with chitosan show better adhesion and also better wound healing process in vivo. Nagiah et al. developed P3HB coaxially electrospun fibres coated with gelatin. From their research can be reported that during in vitro degradation, both surface and bulk erosion was observed. It was managed to point to the resistance of the P3HB fibres, and their good thermal stability was shown too. Chen GQ, Wu Q. reported a study in which they test both PHB and PHBV in the form of films with various types of cell cultures. In the results they conclude that both materials exhibit high levels of cell adhesion and are suitable for producing matrices for in vitro proliferation tests [32, 33].

2.4 Wound healing with the use of a wound dressing

This section of the theoretical part will concentrate on wound dressings based on P3HB as one of the future applications of the acquired knowledge from this Master´s thesis.

2.4.1 Natural wound healing process

The human body is constantly affected by various external factors. Therefore, there is a function of human skin as a barrier. If the skin becomes injured, the healing process, usually divided into three (some literature references state four) stages, begins. First of all, the body starts the process called hemostasis, which represents the arrest of bleeding. The body prevents blood loss by keeping the blood within the blood vessels. Basically, hemostasis occurs through two processes - temporary blockage of the injured site by a platelet plug and blood coagulation or creation of intricate network of polymerized fibrin protein (clot formation). The result of these processes is the closure of the injured vasculature until the tissues heal [34, 35].

In the second phase, the body elicits an inflammatory response that involves several reactions. During the inflammation, a blood clot is formed. Subsequently, the white blood cells (leucocytes) are accumulated (the accumulation process is called influx) at the injury site, which causes the ingestion of bacteria and other foreign particles in the injury. The cellular debris is also cleaned up by these so called 'cell-eating leucocytes' [6, 36, 37]. The inflammatory reaction is ended by wound debridement, which represents removing dead (necrotic) or in some way infected skin tissue. The onset and course of wound debridement depend on many factors, especially on the type of wound [38].

The healing process continues with the subsequent phases, which are cell proliferation and remodelling. All of the stages are straightforwardly described on figure 2.6. Cell growth and their proliferation have an essential role in promotion and acceleration of the wound healing process. The two mentioned processes - inflammation and proliferation - are promoted by growth factors and bioactive components. Thus, most of the wound dressings concentrate on promoting cell proliferation by incorporation some specific substances [39].

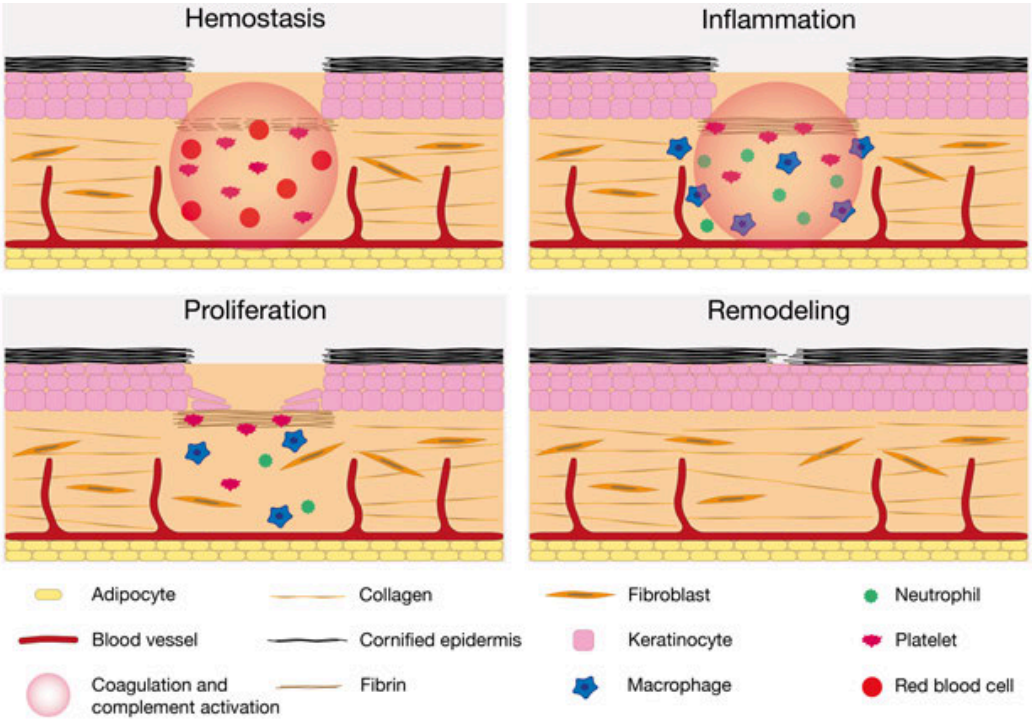

Figure 2.6: Simplified description of all stages of wound healing process (taken from [40])

2.4.2 Characteristics of a wound dressing

Wound dressings are usually applied to chronic or surgical wounds. The usage of wound dressing is an immense advantage because of several reasons. First of all, the wound dressing has the ability to compress the tissue in order to stop the bleeding process. Considering that they are attached to an injured body part, the wound dressings immobilise that body part as a result. They also act as a protection from the environment and soiling with body fluids. Lastly, wound dressings are often used for promoting the wound healing process and decreasing the pain [41].

The wound should be properly treated to avoid wound infections that can significantly impact the whole healing process and its consequences. In some cases, sepsis and even patient death can be the results of an inappropriate healing process. The used wound dressing should meet several requirements, which, if they are meet, characterise the wound dressing as an ideal. The requirements are [6]:

- act as a physical barrier
- be oxygen permeable
- provide a moist environment
- be sterile and non-toxic
- be non-adherent
- maintain a proper tissue temperature.

The above briefly stated requirements are justified in the design of an ideal wound dressing. Various requirements provide specific tasks or functions that are intensely important for the proper and efficient progress of wound healing. Some of the requirements are listed in the table 2.2 with a description of their importance [6].

Table 2.2: Characteristics of an ideal Wound dressing (taken from [6])

Characteristics of Wound dressing	**Importance in Wound healing**
Providing a moist wound environment	Prevents dehydration and cell death Promotes epidermal migration[1] and angiogenesis[2] Maintains moisture at the wound bed
Removal of excess exudate	Exudate[3] is essential for the wound healing process, but excess exudate can cause healthy tissue maceration[4], resulting in a chronic wound.
Allows gaseous exchange	Oxygenation controls exudate levels and stimulates epithelialization[5] and fibroblasts[6].
Prevents infections	Microbial infections delay the wound healing process by prolonging the inflammatory phase and by inhibiting epidermal migration and collagen synthesis.
Low adherence and painless removal	Removal of adherent dressing can be painful and can cause further damage to granulation tissue[7].
Cost effective	An ideal dressing should assure the wound healing process at a reasonable cost.

Short description of the terms used in the table 2.2:

Epidermal migration[1] – epidermal migration represents a mobilisation process of naturally non-mobile epidermal cells, during which they spread across the wound. The process is accompanied by the wound contraction [36].

Angiogenesis[2] – determines the process of blood vessels growing from the existing vasculine [42].

Exudate[3] – wound exudate constitutes a fluid mixture of water, electrolytes, nutrients, inflammatory mediators, white cells, proteases, growth factors and waste products, which include wound exudate itself and possibly dressing degradation products. The presence of exudate with the described composition, especially during acute wound healing (inflammatory and proliferation phases), is vital as it supplies all the nutrients required for healing [43].

Tissue maceration[4] – the definition of maceration of skin around the wound is 'the softening and breaking down of skin resulting from prolonged exposure to moisture' [44].

Epithelialization[5] – represents a process during which epithelial cells migrate upwards and cover and repair the site of the wound (Epithelialization takes place during the proliferation phase) [45, 46].

Fibroblasts[6] – cells called fibroblasts play an essential role in producing collagen, glycoaminoglycans, and proteoglycans (significant components of the extracellular matrix); Fibroblasts provide the restoration of injured tissue [47, 48].

Granulation tissue[7] – is vascularised tissue formed during chronic inflammation, composed of macrophages, fibroblasts and neovasculature. The granulation tissue has two major functions: promoting the growth of further granulations and stimulation of wound contraction [49, 50].

As the new materials and wound dressings, in general, are developing, new demands on wound dressings arise. Several of them are biodegradability, bioabsorbability (the ability to be absorbed through the bioabsorption process whereby substances are absorbed by the tissues and organs of organisms) and flexibility. In addition, the manipulation with the wound dressings and their application must be uncomplicated [51].

2.4.3 Wound dressing types

Wound dressings could be divided into two groups – traditional ones and modern ones. Traditional wound dressings try to fulfil primary requirements such as keeping the wound dry and warm, including an absorbent pad and act as a physical barrier from the environment. However, the traditional wound dressings have one significant deficiency. Their adherence to the human body causes serious difficulties and real trauma to the patients. In recent, as the market potential of wound dressings increased, the traditional wound dressings were developed, and their properties were improved and refined. The impregnation of paraffin onto the gauze or coating viscose fibres with polypropylene can be named as examples [51].

Nevertheless, the mentioned traditional wound dressing types still do not meet the complex requirements for the ideal wound dressings. For this reason, it is essential to concentrate on developing new methods and materials for producing wound dressings. Several of the modern wound dressing types with their advantages and disadvantages are listed below in the table 2.3:

Table 2.3: Overview of advantages and disadvantages of different types of wound dressings (taken from [6])

Type	**Advantages**	**Disadvantages**
Sponges	• high porosity • thermal insulation • sustain a moist environment • absorb wound exudates • enhance tissue regeneration	• mechanically weak • may provoke skin maceration • unsuitable for third-degree burn treatment or wounds with dry eschar
Hydrogels	• high absorption properties • provide a moist environment at the wound site • water retention • oxygen permeability • ensure the solubility of growth factor/antimicrobial agents	• weak mechanical properties • need for a secondary dressing
Hydrocolloids	• non-adherent • high density • painless removal • high absorption properties	• can be cytotoxic • have an unpleasant odor • low mechanical stability • maintain acidic pH at the wound site
Films	• impermeable to bacteria • allows the healing process to be monitored • painless removal	• hard to handle • non-absorbent • adhere to the wound bed and cause exudate accumulation
Membranes	• act as physical barriers • membranes simulate extracellular matrix (ECM) structure • assure gas exchange, cell proliferation, and nutrient supply	• the materials and solvents used in the production • process may be harmful
Fibers	• non-adherent • high porosity and absorption capacity • mimic the skin´s extracellular matrix	• unsuitable for third-degree, eschar, and dry wounds • if the wound is highly exudative, need a secondary dressing

Both fibres and hydrogels need a secondary dressing for some reasons. Accordingly, their combination could achieve a synergic effect through the association of advantages of both types, and in addition, the fibres can work as a component bringing the required mechanical properties. This assumption will be further investigated in connection with this master´s thesis.

3 Experimental part

3.1 Materials

P3HB (or abbreviated as PHB) in the form of white powder treated using acetone with the product marking 2189 (M_w = 484,000 g/mol, T_m = 173 °C) was supplied by Nafigate company.

Chloroform (abbr. as CHF) was provided by Sigma Aldrich as an anhydrous types stabilized by ethanol and amylene respectively.

PEG was provided by the SLOVECA Sasol Slovakia spol. s.r.o. company with the commercial name Slopeg 1000 in the form of white powder, M_w = 1000 g/mol.

PLA Ingeo^{TM} 4060D was provided by NatureWorks LLC in the form of clear pellets; T_g = 55–60 °C (ASTM D3418), T_m = 210 °C.

PCL with commercial name CAPA^{TM} 6500 was provided by company Ingevity in the form of white pellets, M_n = 50,000 g/mol, T_m = 58–60 °C.

Syncroflex^{TM} 3114-LQ-(GD) (abbr. SYNC) (oligomeric adipate ester) was provided by CRODA Europe LtD as a yellow oily liquid, dynamic viscosity 3000–3500 mPa · s at 25 °C.

Acetyltri-n-butyl Citrate (Synonymes A4 or ATBC) with commercial name Citroflex® A-4 was provided by Vertellus LLC in the form of clear, oily liquid;
molecular formula $C_{20}H_{34}O_8$; density 1.048 g/cm^3 at 25 °C.

EMERY MC 2192 (abbr. MC) as a liquid polyester fully composed of biobased monomers was provided by Emery Oleochemicals, dynamic viscosity 5000 mPa · s at 20 °C (DIN 53019 - Brookfield method).

Minimum Essential Medium Eagle M4526 (Synonym: αMEM, MEM) in alpha modification with sodium bicarbonate was provided by Sigma Aldrich as a sterile-filtered red liquid, suitable for cell culture.

3.2 Optimization of centrifugal spinning fibres production

3.2.1 Upgrade of polymer solution dosing

For the laboratory preparation of fibres, the machine named FibeRio CycloneL1000 for producing micro and nanofibers utilizing Forcespinning Technology® was used. As described

in the theoretical part, the spinneret in the middle of the equipment is specialized for 2 ml of polymer solution, injected directly into the spinneret before each cycle.

In order to achieve better handling and faster fibre production, it has been proposed to change the existing intermittent dosing system to continuous. The dosing syringe containing the polymer solution was connected to a syringe pump (LAMBDA VIT-FIT (HP) Syringe Pump –Infusion Pump, shown in the Figure 3.1) located outside of the spinning device to ensure a constant dosing rate. The syringe pump (Figure 3.2) moves forward at a pre-set speed to evenly discharge a given amount of solution into the dosing hose. The polymer solution was then moved into the device's interior via the dosing hose, where it was dosed directly into the spinneret via a wide needle during the spinning period before the stepper motor was turned off. Figure 3.3 shows an inside view of the spinning system with the dosing hose attached to the wide dosing needle pointing to the head.

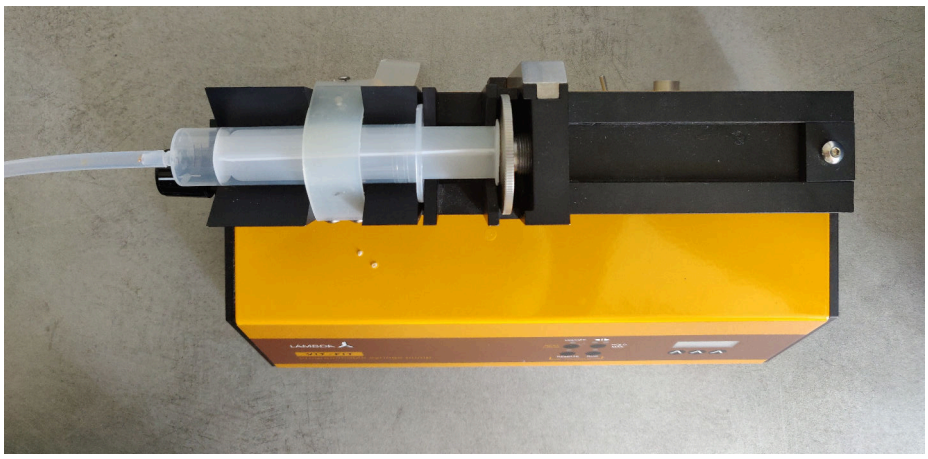

Figure 3.1: Top view of a syringe pump with the dosing syringe

Figure 3.2: Front view of a syringe pump with the set feed rate

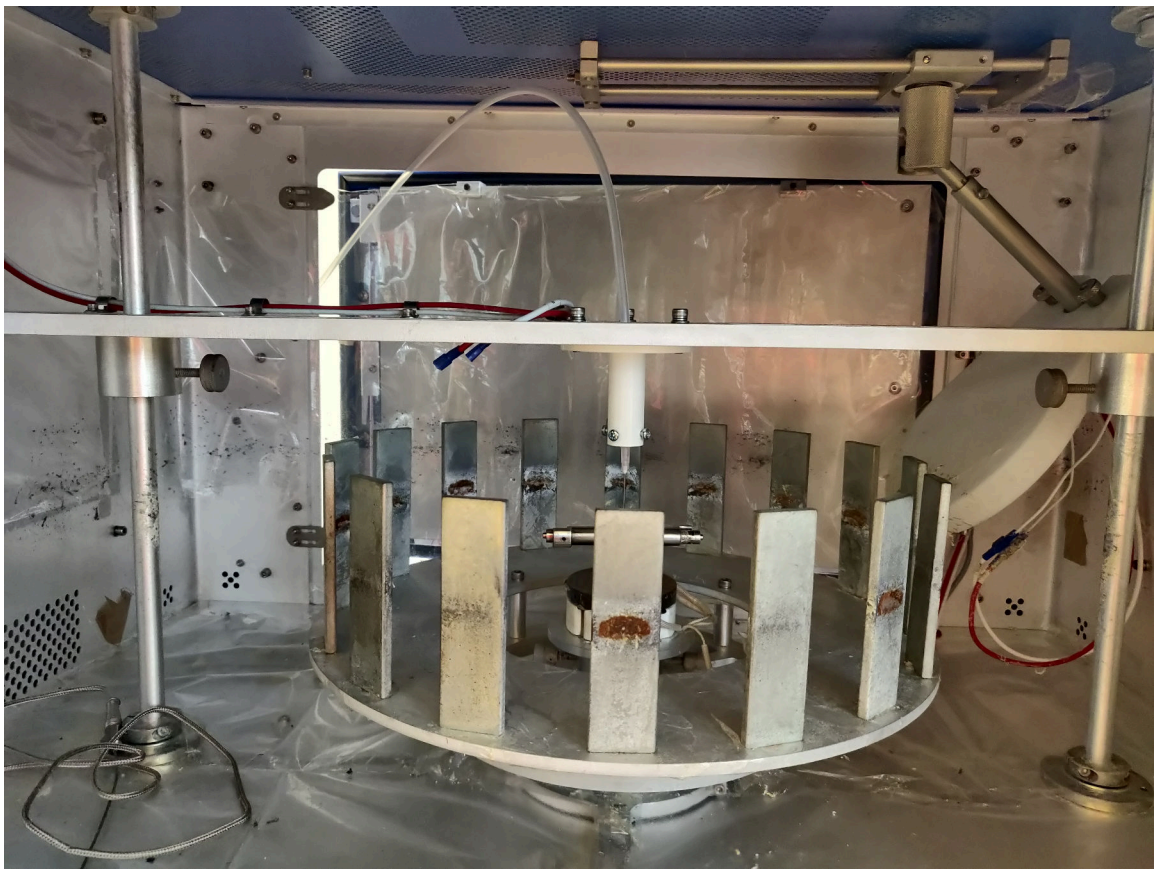

Figure 3.3: Front view of the inside of the spinning device with the optimized dosing system

3.2.2 Processing parameters

The optimisation of processing parameters is essential to produce fibres. It is feasible to accomplish fibre preparation reproducibility through uniformly defined process parameters and detect another parameter's instability if reproducibility is not achieved. Determining the optimal process parameters for spinning individual solutions also serves to compare them with each other.

The process parameters monitored and optimised in this work were: rotational speed, needle diameter, dosing speed and collector distance. Depending on the properties of solution especially its viscosity and spinning ability, the dosing speed and rotational speed were varied. The dosing speed on a syringe pump was set to 100 (which corresponds to 10.0 % of full rotational speed) for most samples and 50 (5 %) for the remaining ones. A polymer solution dosing speed of 50 corresponds to 40 ml of the polymer solution delivered in 90 seconds, representing the duration of one spinning cycle.

The rotational speed of the spinneret was varied from 4,000 to 14,000 revolutions per minute (abbreviated RPM). The 30G needles with outer diameter of 0.3 mm were used for majority of the experiments. Some solutions, however, required spinning with 27G needles with a 0.4 mm outer diameter. Additionally, the effect of needle diameter on the resulting fibres diameter was also investigated using 25G needles with a 0.5 mm outer diameter. After every three runs, the needles were replaced with new ones.

For most samples, the collectors were placed at a distance of 130 mm from the spinneret. The collector distance was changed in a trial that assessed the effect of the collector distance on the polymer solution spinnability. The total number of collectors present during spinning cycles was 16, and all had the same dimensions: $11.5 \times 3.2 \times 0.7$ cm.

3.2.3 Chemical composition of solution

Preparation of P3HB solutions in chloroform with different concentration

Several solutions were prepared for the first experiments on the centrifugal spinning machine by dissolving the P3HB powder in chloroform at four concentrations – 3, 5, 7 and 10 wt.% Ethanol was the chloroform stabiliser. The choice of concentration was based on the literature review and experiences gained while working on a bachelor's thesis. The solutions were prepared by mixing appropriate amounts of P3HB and chloroform (table 3.1) and heating in a water bath at 58 °C for 80 min in a closed boiling flask to prevent the chloroform evaporating. The temperature was set slightly below the boiling point of the chloroform to reach complete dissolution of polymer and at the same time prevent the creation of overpressure inside of the closed boiling flask. When the whole amount of P3HB was dissolved, the preparation was complete.

Table 3.1: The required amounts of P3HB and chloroform for preparation of polymer solutions

Solution concentration (wt.%)	**P3HB** (g)	**Chloroform (ml)**
3	6	130.2
5	10	127.5
7	14	124.8
10	20	120.8

The viscosity of each solution was determined after the solutions were prepared and cooled down. The viscosity measurement was always performed directly after polymer solution preparation and after the preparation of fibres.

Preparation of P3HB solutions in chloroform with different chloroform stabilizer

To prepare the polymer solutions for centrifugal spinning, the chloroform was used as a solvent. The effect of a chloroform stabiliser on the prepared solution's stability and the properties of fibres made from the polymer solution was investigated. The compared stabilisers were amylene and ethanol at widely available concentrations.

Preparation of P3HB solutions in chloroform with a few other biopolymers

The solutions with the concentration of 5, 7 and 10 wt.% were modified by making blends with a few other biopolymers. For this purpose, it was decided to use polyethylene gly-

col (PEG), polylactic acid (PLA) and polycaprolactone (PCL). The ratio of P3HB to other biopolymer was suggested as 70:30 since the microfibres should be based on P3HB, and the 30 wt.% of the other biopolymer is sufficient to see some changes in production or properties of fibres. The modification in fibres processing and fibres properties based on the presence of another biopolymer was observed.

Preparation of P3HB solutions with addition of plasticizer

A change in the chemical composition of the polymer solution was also studied by the addition of a plasticiser. The intention was to determine whether applying the plasticiser directly to the polymer solution could increase the strain of the fibre structures created by centrifugal spinning technology. Based on previous work dealing with modification of P3HB by plasticiser in the melt, three potentially working types of plasticisers were selected - Syncroflex, Citroflex A4 and EMERY MC 2192. The amount of the plasticisers added to the solution was 5, 10 and 15 wt.% based on the weight of P3HB used.

3.3 Characterization of centrifugal spinning fibres production

3.3.1 Gel permeation chromatography

Gel permeation chromatography is an analytical method based on differences in the molecular weights of individual samples, provided that the difference in molecular weights is significant. Separation of the individual fractions of the sample based on their molecular weight is performed using a porous swollen gel. The principle is that the low molecular weight fractions are caught in the pores of the gel and retained in the system for a more extended period of time. The high molecular weight fractions, on the other hand, do not fit into the pores of the porous gel, which causes them to pass through the system without much delay [52].

The decrease in the molecular weight of P3HB powder was determined by measuring it over time. As the molecular weight influence the spinnability and fibres properties, it was essential to know the value.

Firstly, the P3HB powder was dissolved in chloroform stabilized by ethanol and diluted to a 3–6 µg/ml concentration. The GPC analysis was performed on Agilent Technologies HPLC series 1100 chromatograph with PLgel mixed-c 5 µm, 7.5×300 mm column, with chloroform as the mobile phase. Linear polystyrene standards with narrow distribution were used for calibration.

3.3.2 Viscosity measurement

The viscosity of a polymer solution directly relates to the molecular weight of the polymer. Polymers with a high molecular weight increase the viscosity of the solvents in which they dissolve significantly. Increased polymer viscosity is caused by strong internal friction between arbitrarily coiled and swollen macromolecules and the surrounding solvent molecules.

In reality, the higher the viscosity, the higher the molecular weight of the polymer, but the correlation is not straight [53, 54].

The viscosity of the polymer solution was directly measured after it was prepared directly and furthermore after the fibres were produced. The aim was to capture how the viscosity of the polymer solution changed. The viscosity was determined using a Brookfield RVDV-II+PX rotational viscometer, which was calibrated first on a standard oil with a known viscosity 4955 cP. For most of the measured solutions, the measurement was carried out by the laboratory temperature with 50 ml of the polymer solution using spindle number 6.

3.3.3 Parameters reflecting spinnability

Spinnability is defined as the quality of being suitable for spinning or the capability to be spun (used of fibres) [55]. The polymer solution spinnability was assessed based on several parameters, which were evaluated visually during the formation of the fibres and at the same time after their preparation. The observed parameters may include:

- the weight of fibres formed
- the rate of fibre formation during a given spinning cycle
- the presence of beads
- the stickiness of the formed fibres
- the formation of a bulky cocoon of fibres in the whole space among the collectors.

After each spinning cycle, the prepared fibres were removed and weighed on analytical balances. The weights of the individual fibre cocoons were compared with each other. To confirm or rule out the possibility of reproducible fibre output under predetermined conditions, the spinning cycle was repeated at least five times under the same conditions.

3.3.4 Thermogravimetric analysis

Thermogravimetric analysis (TGA), as one of the thermal analysis methods, measures the change in weight of the sample as a function of temperature (scanning mode) or time (isothermal mode). Thus, the processes of desorption, absorption, sublimation, evaporation, oxidation, reduction and decomposition can be monitored by TGA. However, thermal processes that are not associated with a change in sample weight (melting, crystallisation, glass transition) cannot be determined by TGA. The measurement is carried out in an inert (mostly nitrogen) or oxidising (air or oxygen) environment. The analysis yields a TGA curve, which is a graphical representation of the change in sample weight (wt.%) as a function of temperature (°C) or time (min) [56].

Prepared fibres, individual pure materials as a reference (PHB, PLA, PCL, plasticizers), and foils produced by slow evaporation of the solvent from the solutions used for fibre preparation were all subjected thermogravimetric analysis. A small cut piece of the foil or a small cluster of fibres placed in an aluminium pan was used to carry out the measurement. The weight of the individual samples utilized for the analysis ranged in weight from 15 to 30 mg.

The measurement was performed on a TGA Q500 instrument from TA Instruments in nitrogen and an oxidizing atmosphere. The temperature program for sample analysis was set as follows: equilibrate to 40 °C, isothermal at 40 °C for 1 min, heating to 500 °C at a rate of 5 °C/min, transition to an oxidizing atmosphere, heating to 550 °C at a rate of 10 °C/min, cooling to room temperature.

3.3.5 Differential scanning calorimetry

The DSC method is based on measuring enthalpy changes that the material absorbs or releases into the environment because of chemical, physical or biological processes. These changes can be divided into endothermic (heat is consumed), which can include melting, evaporation and glass transition, and exothermic (heat is released), which in turn includes crosslinking, crystallization, or chemical decomposition. All these processes are then represented by a deviation from the baseline of the DSC curve, which otherwise represents a constant value of heat flux Q. The measurement is suitable, for instance, for recognizing materials and their blends, for determining the glass transition temperature, the melting point and for calculating the crystallinity [57].

Analysis was carried out with approximately 10 mg of material of appropriate dimensions placed in an aluminium pan. The samples were measured on a DSC 2500 (TA Instruments, New Castle, DE, USA) and analysed in a nitrogen environment with a flow rate of 70 ml/min with the following temperature regime:

The measurement was initiated by tempering to −30 °C (in the case of PCL analysis alone, the temperature was reduced to −70 °C) with a residence time of 1 minute. Heating was performed at a rate of 10 °C/min to 200 °C for 1 minute, after which cooling to −30 °C was selected, and the whole cycle was repeated in the same manner. Finally, the temperature was lowered to 30 °C.

3.3.6 Scanning Electron Microscopy

The scanning electron microscope scans with an electron beam over the observed sample and creates an image by detecting low energy secondary electrons emitted from the sample's surface. The microscope was used to examine the structure and morphology of prepared fibres. The diameter of the fibres and the presence of beads on the fibres were also measured and compared [58].

The prepared fibres were observed with a ZEISS EVO LS 10 microscope. Polaron gold was used for gilding all the samples, and the gilding took place in manual mode by combining gold and palladium (duration 60 s). Argon with a purity of 99.996 was used as a gilding gas. The voltage was 1.5 kV, current 14 mA. Gold-plated samples were scanned in secondary electron (SE) mode.

3.3.7 Confocal Laser Scanning Microscopy

Confocal Laser Scanning Microscopy (CLSM) represents a combination of an optical imaging microscope and a point scanning by a monochromatic laser beam. The CLSM can create 2D and 3D images of the surface with the advantage of not requiring prior surface

preparation, and in comparison to the SEM, it is not limited in terms of scanning range [59].

Fibres were observed on the CLSM LEXT OLS 3000 microscope using 5x, 10x, 20x, 50x type of objective. Samples were analysed under upper exposure with half of the light intensity, bright filter and without polariser. An adhesive tape was utilised to mount the samples on an specimen stage.

The software of the CLSM microscope was also used to provide an analysis of the fibre diameter. The analysis was made using the measurement of the distance between two points. A minimum of ten fibres was selected for measurement; each fibre was only measured once.

3.3.8 Tensile test

The tensile test is one of the static testing methods of mechanical properties. It is possible to determine the effect of tensile deformation, from which the strength of the material is evaluated, test sample that was made of the given material, respectively. Suppose the dimensions of the test samples are readily measurable and given by a norm; the result of the measurement is a tensile curve, which shows the dependence of the applied stress σ on the relative deformation ϵ. The linear region of this curve is used to determine Young's modulus of elasticity E, which is characteristic of each material. The curve further provides information on yield strength, tensile strength, or elongation. The resulting tensile curve can have a different shape depending on the type of material. Materials that behave brittle show high strength values without the presence of yield strength and very low ductility. On the contrary, tough polymers achieve the highest values of ductility among the measured materials [60].

The tensile test was performed on samples in the form of planar strips, which were cut from planar substrates manufactured by the company Nano4Fibers. The strips were cut manually on a manual sample cutter (figure 3.4a, which is in detail showed in the figure 3.4b), and the strips thus prepared had dimensions (38 $\times$ 5.3) mm. At both ends of the cut strips, space was created to properly hold the sample between the wedge grips of the test device. The tested samples are shown in the figure 3.4c. The thickness of the individual strips was measured using a micrometre. Since the thicknesses of the individual planar substrates varied at various places, the calculated force dependencies on the relative elongation of the sample were related to a specific thickness to make the samples comparable.

The cut specimens in the form of strips were tested on universal test equipment ZWICK Z 010. A 10 N load cell was used for the force measurement and 10 N wedge grips was used to hold the specimens. Initial distance between clamps was set to 20 mm and considered as the initial length of tested sample. Before the actual measurement, the input values - the thickness of individual samples - were entered into the software. All samples were measured at a speed of 10 mm/min. The test was terminated by software when the applied force reached 80 % its maximum value.

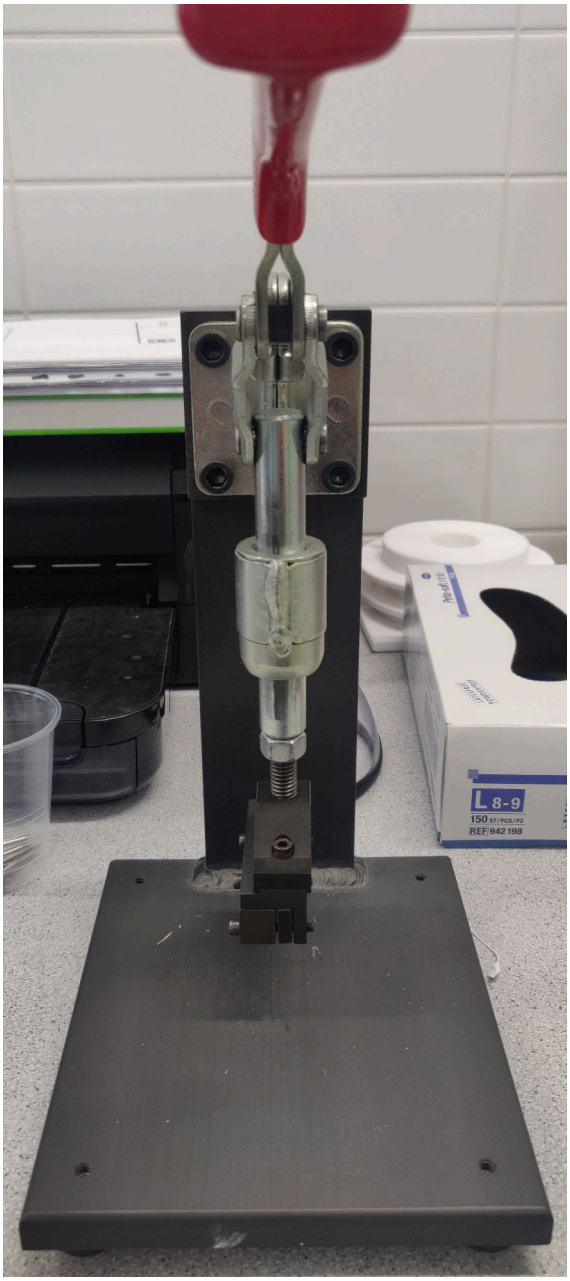

(a) Device for manual samples cutting in the form of thin strips with dimensions (38 × 5.3) mm

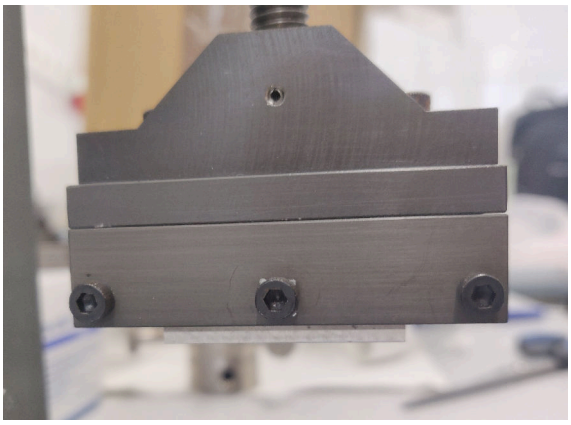

(b) Detailed view on the cutting part of the device

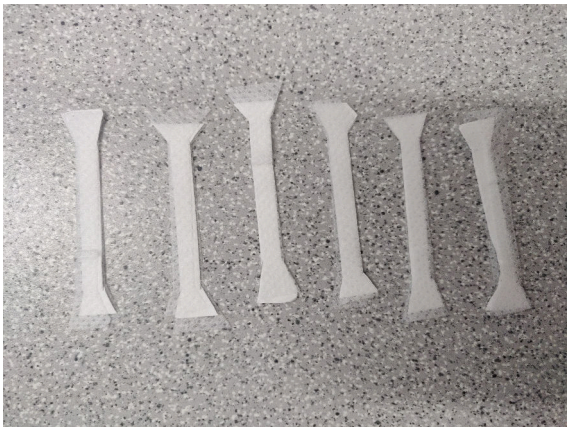

(c) Samples produced by device for manual strips cutting with an additional material on both size for successful holding the sample between the wedge grips

Figure 3.4: Device for manual cutting the samples in the form of strips with dimensions (38 × 5.3) mm and the produced samples used for tensile test

3.3.9 Biological properties (cell viability, proliferation and differentiation)

Scaffold preparation and Manipulability test

The manipulability test aimed to determine for both forms of laboratory prepared fibres (cotton like and planar) whether it is possible to prepare disk-like samples required for

biological tests and ascertain if the samples are dimensional stable in water and if the manipulation with those samples in well plates are possible without sample damage.

Demanded disk-like samples with diameter of 6 mm were cut from both mentioned above forms of fibres. The cutting was made manually with a steel punch with a corresponding inner diameter. The prepared disk-like samples were placed in a test plate with 96 wells. Their position was several times changed in order to see how the static charge makes handling difficult. The 3 drops of culture medium were added to the samples in wells (Figure 3.5) to exclude strong hydrophobicity. Samples with the following designation were used for testing (Table 3.2):

Table 3.2: Identification and description of the form of fibres used to test the samples manipulability

Sample number	**Sample name**	**Sample form**
1	Planar10gsm_PHB	planar
2	Vata30G_PHB	cotton-like

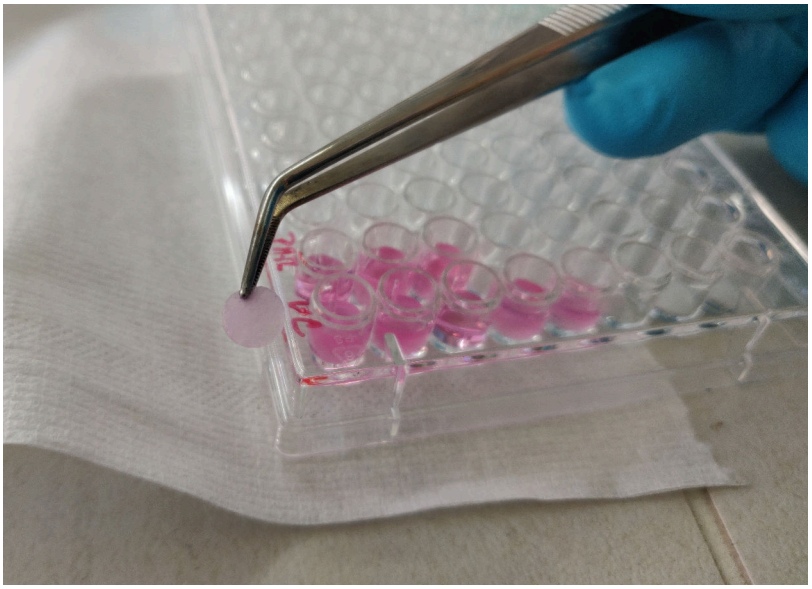

Figure 3.5: Manipulation test with prepared disk-like samples placed in wells of a test plate covered by three drops of culture medium to improve handling with the samples

Scaffold seeding

The procedures deals with cell cultures were performed by cooperating Institute of Experimental Medicine of CAS, Department of Tissue Engineering. Scaffolds with a diameter of 6 mm in 96-well plates were sterilized using ethylene oxide. A culture medium (20 µL drops) was put on the bottom of the wells, where scaffolds were subsequently added. The culture medium contained Dulbecco's Modified Eagle's Medium (DMEM, Sigma Aldrich) enriched by 10 % fetal bovine serum (FBS; Gibco) and 1 % of antibiotics (100 U/mL peni-

cillin and 100 µg/mL streptomycin; Sigma Aldrich). Because of the hydrophobic nature of some scaffolds, another 20 µL of culture medium was added to all the tested groups. The samples were incubated at 37 °C for 30 min. Afterwards, scaffolds were seeded by 2×10^4 of 3T3 fibroblasts (ECACC) in 30 µL of culture medium per well. Cells were left to adhere for 2 hours; then, the medium was fill up to 250 µL per well. Cell-seeded scaffolds were cultured for 7 days in a humidified incubator at 10 % of CO_2 and 37 °C. The cultured medium was changed on day 3. Simplified scheme of biological testing of scaffolds is shown in figure 3.6.

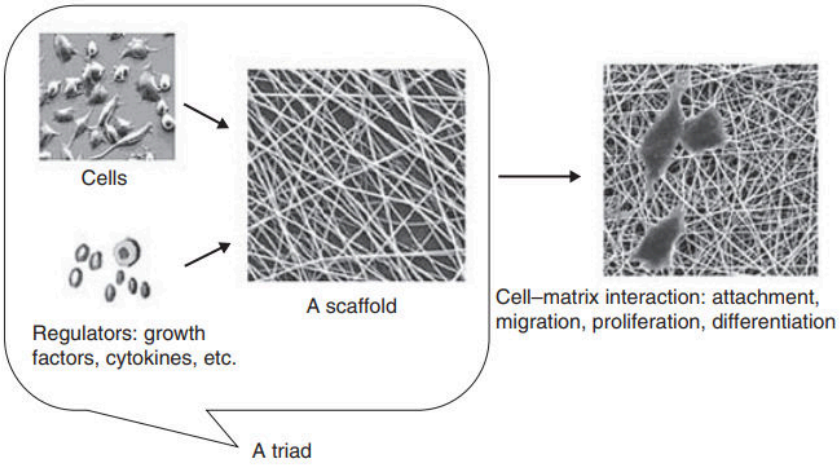

Figure 3.6: Simplified scheme of biological testing of scaffolds (taken from [61])

Cell viability analysis

MTS assay (CellTiter 96® AQueous One Solution Cell Proliferation Assay; Promega) was used to probe cell metabolic activity. Samples were transferred to clean 96-wells to avoid measurement of cells growing on the bottom of the well. MTS solution (20 µL) and 100 µL of the fresh medium were added to the wells with scaffolds or with the control 3T3 fibroblasts seeded on the bottom of the well. The microplate was incubated at 37 °C for 2 hours. The MTS substrate is metabolized by mitochondrial enzymes to violet formazan, which absorbs light at 490 nm. The absorbance of the solution (100 µL) was read in clean microplates using a microplate reader (Infinite M200 PRO, Tecan, Switzerland) at 490 nm and reference wavelength 690 nm. The absorbance of scaffold without cells incubated with MTS substrate was subtracted from the values.

Cell proliferation

Quantification of DNA was used to determine cellular proliferation. The samples were analyzed using Quant-iT™ dsDNA Assay Kit (Life Technologies). After MTS measurement, the scaffolds were put in 200 µL of cell lysis solution (0.2 % v/v Triton X-100, 10 mM Tris (pH 7.0), and 1 mM EDTA) and lysed by freeze-thawing (3 cycles with rough vortexing). For analysis, 20 µL of cell lysate from samples was added to 200 µL of reagent solution, which is bind to double-strand DNA of cells and emits a fluorescence signal. The fluorescence

intensity was recorded on a multimode fluorescence reader (Infinite M200 PRO, Tecan, Switzerland; λex = 485 nm, λem = 523 nm). The fluorescence of the scaffolds incubated without cells was subtracted from the measured values. Results were evaluated using the calibration curve of the standards in the kit.

Cell distribution

Cell distribution on the fibrous scaffolds was detected using confocal microscopy. Samples were fixed with frozen methyl alcohol (−20 °C) for 10 min. Subsequently, the fluorescent probe 3,3'-diethyloxacarbocyanine iodide ($DiOC_6(3)$, Invitrogen, 1 µg/mL in PBS (pH 7.4)) was added and incubated with the samples for 30 min at room temperature to visualize the intracellular membranes. Afterwards, cell nuclei were stained using propidium iodide (PI; 5 µg/mL in PBS, 10 min; Sigma Aldrich), which is intercalated into cell DNA. The scaffolds were washed with PBS and visualized using confocal microscopy (Zeiss LSM 880 Airyscan). Used wavelengths were λex = 488 nm and λem = 520 nm in the case of $DiOC_6(3)$ and λex = 560 nm and λem = 580 nm in the case of propidium iodide.

Statistics

MTS assay and DNA quantification were performed on 6 independently prepared samples. Because of the variability of the measured results, margin values were not included. Nevertheless, at least 4 samples were used for the statistic evaluation. Quantitative data are presented as mean values ± standard deviation (SD). Results were evaluated statistically using SigmaStat 12.0, Systat. If the data passed the normality test and the test of equality of variances, statistical significance between a pair of groups was determined by ANOVA test and Tukey's comparative test for posthoc analysis. If the data were without normal distribution, statistical significance between a pair of groups was determined using Kruskal-Wallis One Way Analysis of Variance on Ranks and Dunn's multiple comparisons test for post hoc analysis. All results were considered statistically significant if p was <0.05.

4 Results and discussion

In the following chapter, the relevant results obtained during the work on the submitted Master´s thesis will be presented and discussed.

4.1 Optimization of spinnability of P3HB solutions

The tables 4.1 and 4.2 provide a detailed description of fibres formed using P3HB solutions with three different concentrations spun at three different rotational speeds. The appendix A lists the SEM images of the individual fibres compared as part of the optimization, which gives a better overview of what the fibres looked like. Table 4.1 presented a description of symbols used in the table 4.2.

Table 4.1: Description of symbols used in the table 4.2

I	II	III	IV	V	VI
Porosity	Fiber shape	Beads count	Impurities count	Cluster count	Rating

Table 4.2: Screening of fibres preparation by three different rotational speed of the spinneret using P3HB solutions with three different concentration

	3 wt.%		5 wt.%		7 wt.%
			4000		
I	not recognized –> fibres are not porous	**I**	little evidence about porosity at some places	**I**	clusters are a little bit porous
II	several fibres connected together	**II**	separated long fibres without much clusters	**II**	separated long fibres with some clusters
III	barely	**III**	not recognized	**III**	not recognized
IV	few	**IV**	barely	**IV**	barely
V	repeatedly	**V**	rarely	**V**	rarely (just small ones)
VI	nice fibres with many clusters	**VI**	separated fibres without impurities	**VI**	similar as 5 wt.% 4,000 RPM

			5000		
I	clusters are highly porous (many big pores), fibres not	**I**	fibres and clusters are not porous	**I**	not recognized
II	separated, but many of them are conglomerate	**II**	many separated thin fibres, wrapped around themselves	**II**	separated long fibres
III	much more than 3 wt.% 4,000 RPM	**III**	few	**III**	not recognized
IV	often	**IV**	more than 5 wt.% 4,000 RPM	**IV**	rarely
V	more than 3 wt.% 4,000 RPM	**V**	just a few small ones	**V**	not recognized
VI	samples are not homogenous, can not be characterized as a whole	**VI**	twisted and wrapped fibres with many impurities	**VI**	nice fibres
			8000		
I	many pores on clusters and also fibres passing through clusters	**I**	clusters are a little bit porous	**I**	porosity recognized just on places where fibres are connected
II	none separated long fibres	**II**	short thin fibres	**II**	mostly separated fibres with some clusters
III	many	**III**	enormous	**III**	not recognized
IV	many	**IV**	similar as 5 wt.% 5,000 RPM	**IV**	rarely
V	many, but small ones	**V**	many small ones	**V**	not recognized
VI	terrible looking fibres	**VI**	very bad looking fibres	**VI**	unsightly-looking fibres

It is clear from the description of the fibres that there is a relatively narrow window of process parameters for each P3HB solution at which the solution can be successfully spun. The term successful spinning in this method means forming a cocoon of fibres extending over the entire space between the spinneret and the surrounding collectors. Moreover, it should be provided that the fibres are not glued together and are not accompanied by the formation of a large number of beads.

Based on the given results, attention was focused on finding the optimal conditions for each P3HB solution to achieve the formation of a cocoon of fibres, if possible.

4.2 Viscosity measurement

The preparation of a solution of P3HB in chloroform and its properties, especially concerning viscosity, affect the spinning process itself and the reproducibility of the fibre preparation. As differences in viscosity were observed in the preparation of the solutions, which subsequently manifested themselves in the failure of spinning, the issue of the viscosity of the solution was subsequently given great attention.

The results from viscosity measurement of polymer solutions prepared using two different types of chloroform is listed in table 4.4. The values represent the difference between chloroform as a solvent that is either stabilized by ethanol or by amylene.

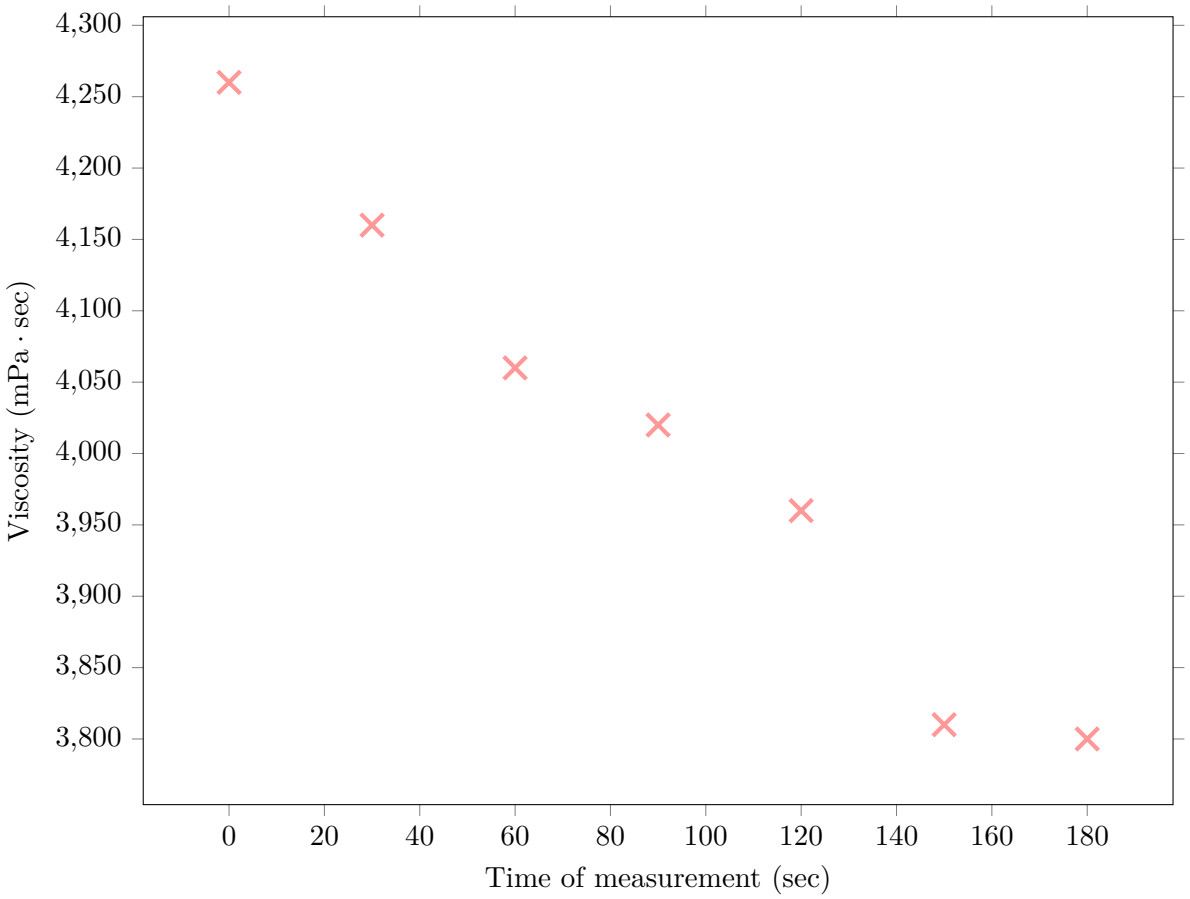

Figure 4.1: The decrease in the viscosity of P3HB solution in chloroform stabilized with amylene as a function of time

Table 4.3: The average values of viscosity of 7 wt.% P3HB solutions (N = 5) in chloroform stabilised by ethanol measured before and after the preparation of fibres to see the viscosity increase

	before	**after**
Average viscosity (mPa · sec)	3828	4420
Deviation (mPa · sec)	168	10
Deviation (%)	4	0

As shown in the figure 4.1, the viscosity of a P3HB solution in chloroform stabilized with amylene is strongly time-dependent. Under the influence of heat and light, chloroform decomposes into toxic phosgene and hydrogen chloride according to the equation 4.1. To prevent this reaction, chloroform is stabilized by either ethanol or amylene, which is, after recovering or drying process, no longer present. It was found that amylene is an ineffective stabilizer in case of P3HB solution since it does not effectively prevent phosgene and hydrogen chloride formation. The hydrogen chloride apparently causes cleavage of PHB chains and therefore the changes of viskosity. Because viscosity is a key parameter in the spinning process, it is impossible to achieve reproducible fibre preparation using this solution [62].

$$2\,CHCl_3 + O_2 \rightarrow 2\,COCl_2 + 2\,HCl \tag{4.1}$$

Table 4.4: The change of viscosity of 10 wt.% P3HB solutions in chloroform stabilised by ethanol and amylene measured before and after the preparation of fibres

Choloform	**stabilised by ethanol**			**stabilised by amylene**		
	before		after	before		after
Viscosity (mPa · sec)	18720	→	19000	7320	↘	2810

The table 4.4 shows the change in viscosity of solutions prepared by dissolving P3HB in chloroform stabilised by ethanol and amylene, respectively. The change in the viscosity value was observed before and after fibre preparation.

In the case of a solution prepared in chloroform stabilised by ethanol, we see a slight increase in viscosity due to the partial evaporation of chloroform. Thus, a slight increase in the viscosity of the solution is associated with an increase in polymer solution concentration. However, a solution prepared in chloroform stabilised by amylene shows a considerable decrease in viscosity, corresponding to the presented dependence in figure 4.1.

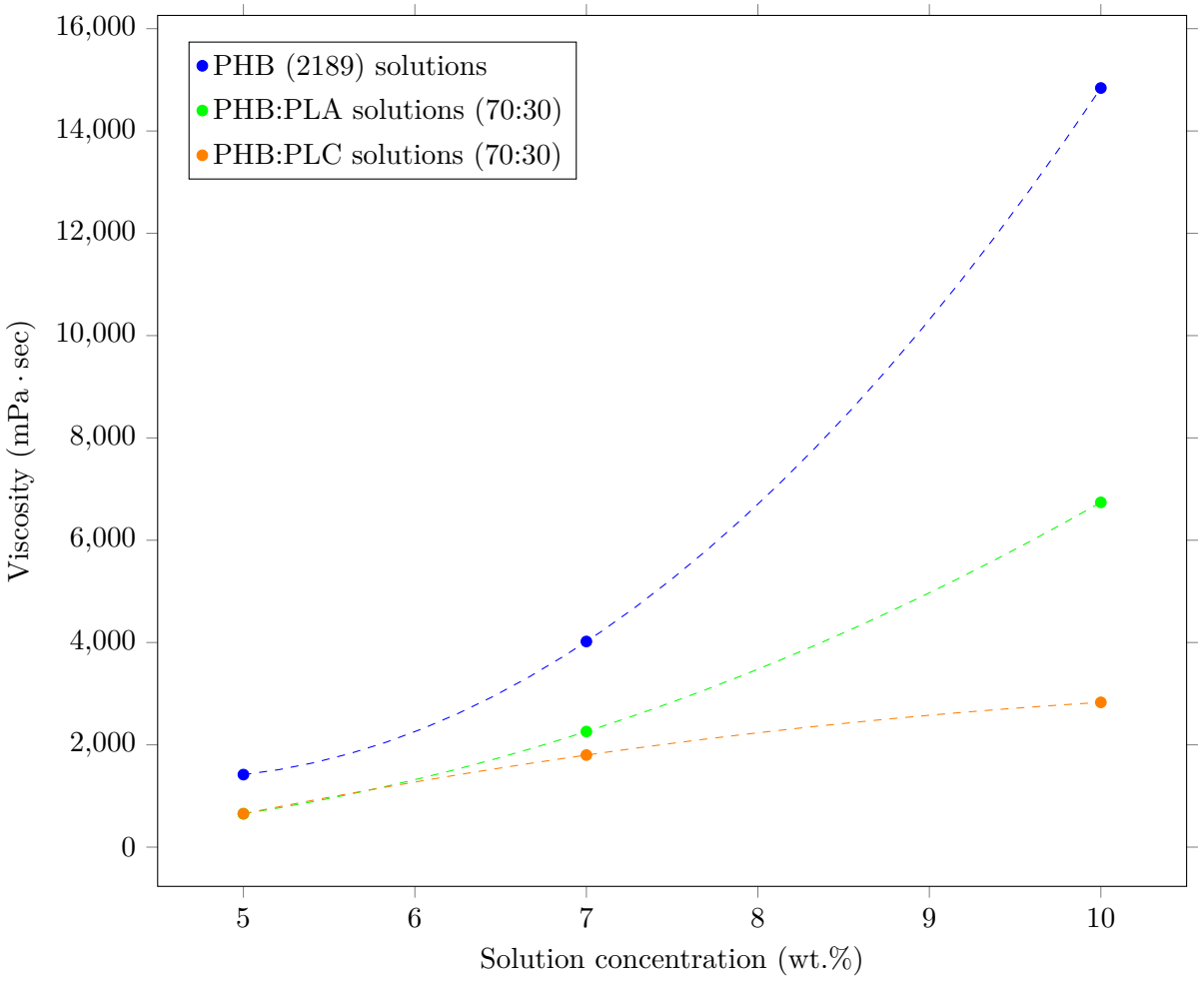

Figure 4.2: The increase in the viscosity of solutions of P3HB, P3HB with an addition of PLA and PCL, respectively in chloroform stabilized with amylene as a function of time

The experimentally measured dependence of viscosity on the solution concentration was used to optimise the properties of the solution. There was a tendency to prepare mixture solutions with the same viscosity value as the solution of P3HB alone. However, it can be seen from the figure that the viscosity of a solution containing exclusively P3HB increases most rapidly with increasing polymer concentration compared to solutions containing 30% PLA and PCL, respectively. In the end, the solutions were not prepared to the same viscosity value, but the process parameters were optimised to spin the solutions even at these viscosity values.

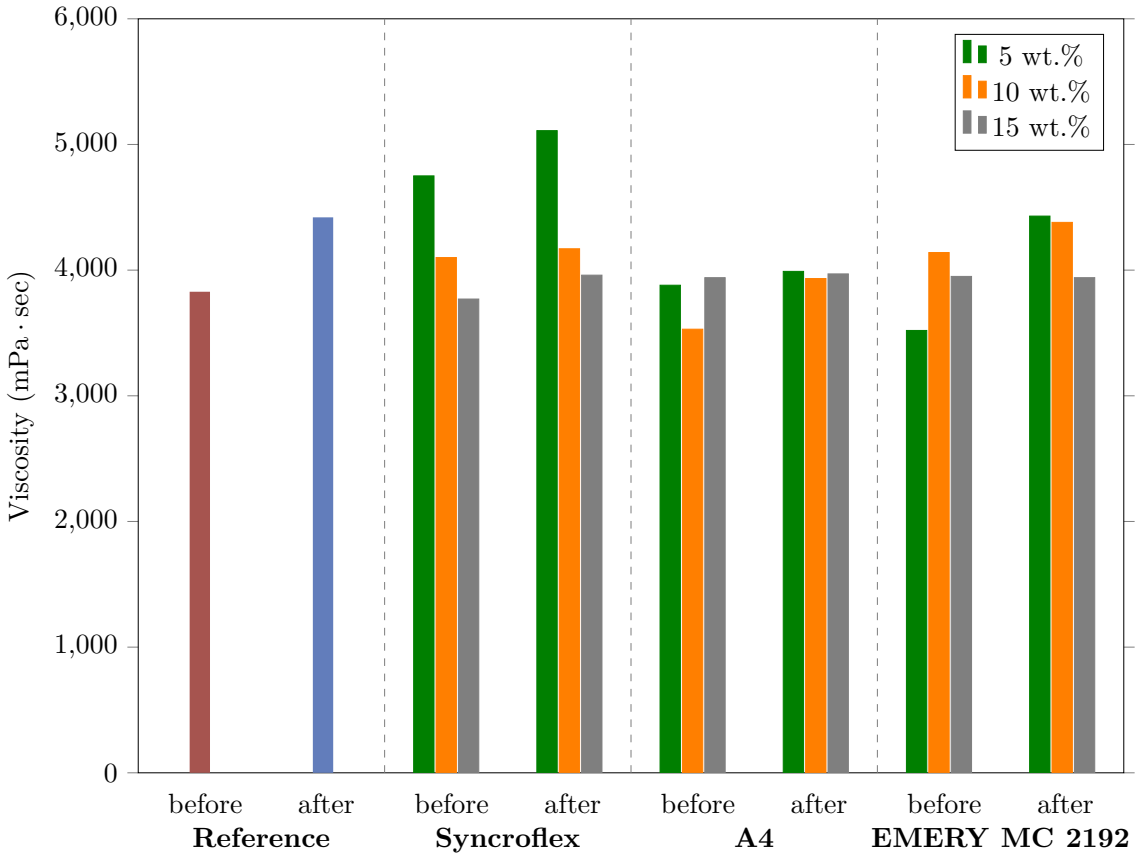

Figure 4.3: Viscosity measurement of 7 wt.% P3HB solutions in chloroform stab. by ethanol - reference, with an addition of 5, 10 and 15 wt.% three diferent types of plasticiser - Syncroflex, A4 and EMERY MC 2192. The viscosity was measured before and after preparation of fibres.

It is evident from the figure 4.3 that the addition of plasticiser did not cause any significant change in the viscosity of the solutions. The only difference was noted for the sample containing Syncroflex. In this sample, it is possible to observe a decrease in viscosity with increasing plasticiser content and an increase in viscosity after fibre preparation, during which a partial amount of chloroform apparently evaporated.

4.3 Influence of molecular weight on brittleness of fibres

The preparation of the first fibres for this work was carried out two years ago. Since the molecular weight of P3HB is not constant over a longer time horizon, this phenomenon was verified by comparing the molecular weight of P3HB in table 4.5. The measured molecular weight distributions of P3HB are presented in appendix C.

Table 4.5: The average values of viscosity of 7 wt.% P3HB solutions (N = 5) in chloroform stabilised by ethanol measured before and after the preparation of fibres to see the viscosity increase

Sample	**Date**	**Mw (g/mol)**
P3HB 2189 powder	08/08/2018	$5.76 \cdot 10^5$
P3HB 2189 powder	08/12/2020	$4.84 \cdot 10^5$

Fibres prepared by centrifugal spinning two years ago show no signs of brittleness, which may be due to the initially relatively high molecular weight of P3HB. Monitoring the effect of a decrease in the molecular weight of P3HB on the ageing and onset of the brittleness of fibres will be the subject of further investigation. A 7 wt.% polymer solution using P3HB powder with a molecular weight of 300,000 g/mol was prepared for the comparison. However, this solution did not reach a sufficient viscosity to spin the solution. The further investigation of the influence of molecular weight will be carried out using P3HB with a higher molecular weight than the mentioned P3HB powder.

The evolution of fibre brittleness over time was observed on the prepared fibres independently of the use of various P3HB molecular weights. After preparation, the fibres were placed in a laboratory drying oven at a preset temperature of 80 °C for 4 hours. Evaporation of residual chloroform should result in the formation or increase in brittleness of the fibres. This assumption could not be confirmed. After drying, the fibres did not show any visible changes in the brittleness properties. The change was observed for fibres containing 30 % by weight of PCL, which appeared to be more elastic after drying.

An interesting finding related to the change in molecular weight is the use of chloroform with a different stabilizer. The figure shows a comparison of molecular weight distributions of P3HB powder analyzed using amylene and ethanol stabilized chloroform. In addition, the figure also shows a comparison of the molecular weights of P3HB analyzed in the form of solutions prepared using chloroform stabilized by amylene and ethanol.

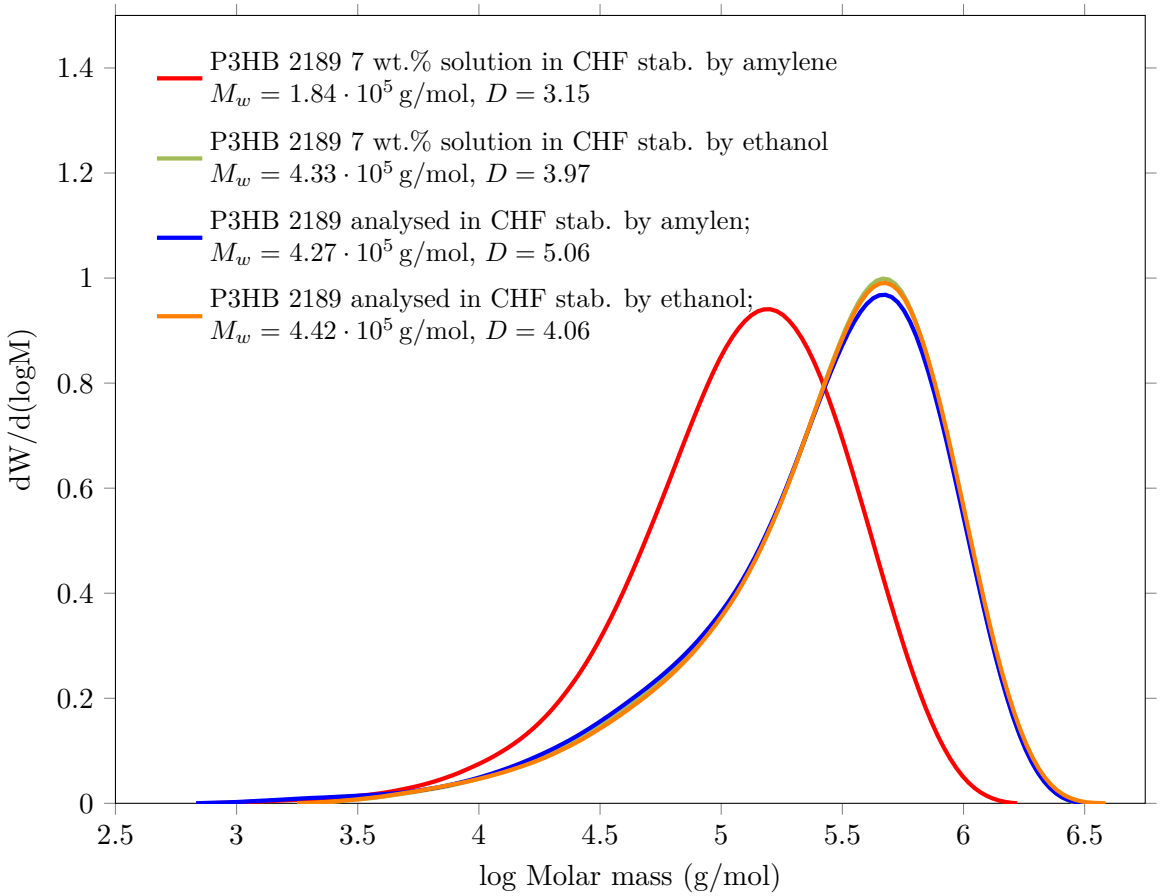

Figure 4.4: The comparison of molecular weight distributions of P3HB analysed in chloroform stabilised by amylene and ethanol and

It is evident from the figure 4.4 that the dissolution of P3HB powder in chloroform stabilized by amylene significantly reduces the molecular weight of the polymer. As a result, the ability to spin a given polymer solution is subsequently affected, which will be discussed in more detail in the following chapter. According to the figure, the result of the GPC analysis itself is not affected by which stabilizer is used for the measurement.

4.4 Influence of chloroform stabiliser on P3HB solutions and prepared fibres

Properties of foils after evaporation a part of chloroform

The foil-forming 7 wt.% P3HB solution prepared using amylene-stabilised chloroform immediately after pouring onto a petri dish began to form droplets and did not remain uniform at all. This subsequently created the impression of interconnected drops, which was also reflected in the richly structured of the resulting foil. However, the strength was satisfying.

The foil prepared using a 7 wt.% P3HB solution in chloroform stabilised by ethanol was smooth, uniform and showed a relatively high degree of elasticity (plasticity respectively) after evaporation of a part of the chloroform.

Properties of foils after evaporation of whole residual chloroform

After evaporation of all residual chloroform, the foil prepared from chloroform stabilised by amylene remained significantly uneven. It also maintained a high strength in those places. However, it reached a relatively high brittleness.

The foil prepared from the P3HB solution with ethanol-stabilised chloroform achieved higher strength than the first type of foil described. However, after the evaporation of chloroform, there was a significant loss of plastic behaviour. Thus, the residual chloroform acted as a temporary plasticiser in the foil.

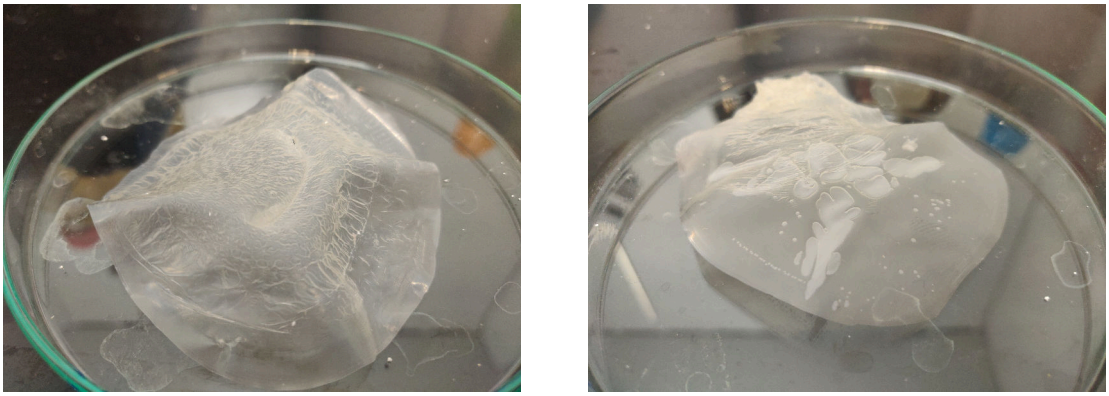

(a) Chloroform stabilised with amylene used (b) Chloroform stabilised with ethanol used

Figure 4.5: Foils prepared by evaporation of chloroform with two different types of stabilisers from 7 wt.% P3HB solution

Spinnability of fibers from 7 wt.% P3HB solution in chloroform stabilised by amylene

The centrifugal spinning of a 7 wt.% solution of P3HB in chloroform stabilised with amylene was carried out with difficulty. Below the rotational speed of 6000 RPM, no fibres could be prepared; the solution flowed out of the top of the spinneret without forming fibres. At a speed of 6000 RPM, it was possible to observe the formation of short, spattered fibres strongly adhered to the collectors. Further increase in speed did not show a significant change in the spinnability of the solution. It was only at 10000 RPM that intact, elastic fibres were formed, but the rotational speed of the spinning head was already so high that a strong air stream was created in the space between the collectors, which entrained the resulting fibres through the gap between the individual collectors.

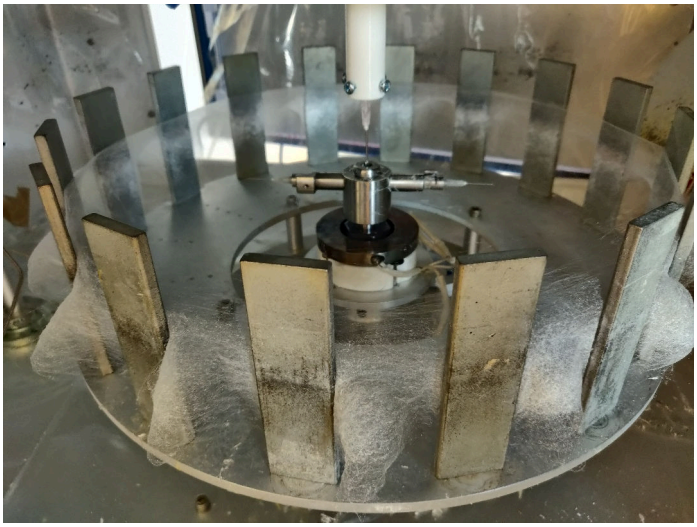

Figure 4.6: Fibres prepared from a 7 wt.% P3HB solution of amylene-stabilised chloroform have been entrained from the space between the spinneret and the collectors by a strong air stream during centrifugal spinning.

Spinnability of fibers from 7 wt.% P3HB solution in chloroform stabilised by etanol

By using a 7 wt.% solution of P3HB in ethanol-stabilised chloroform, it was possible to successfully prepare a bulky cocoon of fibres extending over the entire space between the spinning head and the collectors. However, the stable reproducibility of the preparation of fibres from this solution has not yet been demonstrated.

4.5 Spinnability and reproducibility of fibres preparation

The spinning of P3HB solutions has long been accompanied by the impossibility of creating a higher content of long, non-glued fibres without the formation of beads. The performed optimization described in the chapter 4.1 found the limits of individual polymer solutions with different concentrations of polymer. Examples of stages where spinning was not successful are shown in the 4.7a, 4.7b, 4.7c figures.

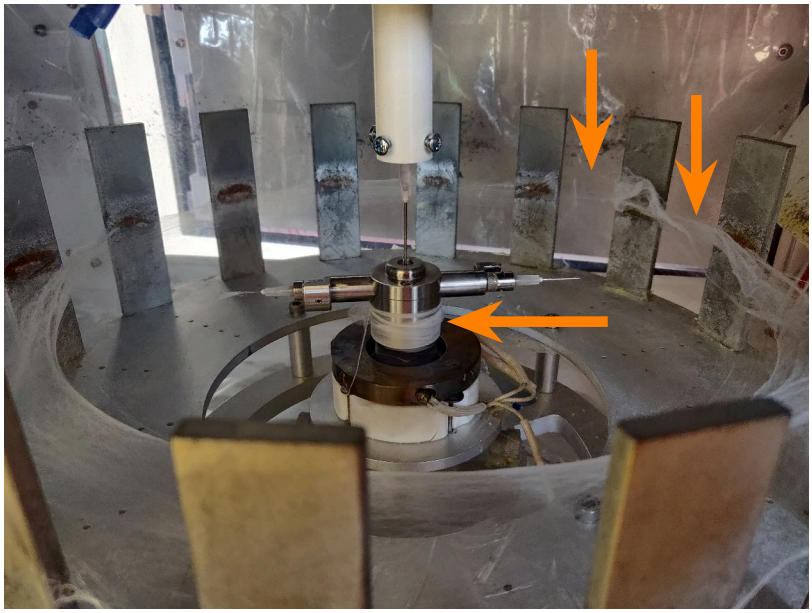

(a) Not efficient centrifugal spinning of a P3HB solution

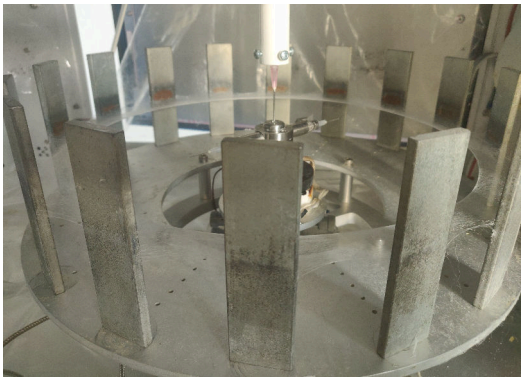

(b) Planar fibrous layer resembling paper

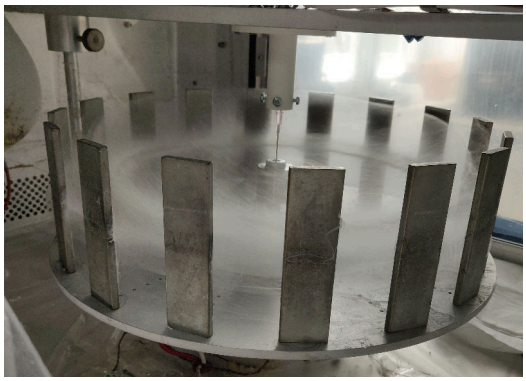

(c) Successfully prepared bulky cocoon of fibres

Figure 4.7: Progress in the preparation of fibres from a solution of P3HB in chloroform by the centrifugal spinning method

A demonstration of centrifugal spinning of solution, which was complicated to transform into fibres is presented in the figure 4.7a. Due to almost impossible spinning of the solution, only a small amount of fibres was formed. Most of them could not adhere to the collectors, due to the their shrinkage were caught with a rotating needle and therefore were finally wound on the spinneret. The second case of unsuccessful preparation of fibres using centrifugal spinning was when the resulting fibres fell into only one plane of the collectors, where over time, they multiplied and glued together, which ultimately created a planar fibrous layer resembling paper (4.7b). Figure 4.7c shows the successful formation of a bulky cocoon of fibres in the entire space among the collectors.

Reproducibility of fibres was analysed based on weight of prepared cocoons of fibres after each cycle of centrifugal spinning. At least 3 cycles for each fibre sample were repeated in order to get some statistical information about the values. Weights of selected prepared cocoons are listed in tables 4.6 and 4.7.

After optimising the dosage (its changes to continuous dosing respectively) while at the same time stabilising the spinning time, the reproducibility of the fibre preparation was verified. The reproducibility was assessed by comparing the weights of the cocoons prepared by re-spinning one polymer solution under the same conditions and the same length of the individual spinning cycles. The cocoons weights of the two selected polymer solutions are listed in tables 4.6 and 4.7 respectively. It is clear from the tables that the deviation between the weights of the cocoons reaches a value below 10%, which can be considered as a reproducible preparation of the fibres.

Table 4.6: Cocoons weights of reference cotton-like samples prepared from 7 wt.% P3HB solution in chloroform stab. by ethanol, 30G needles were used

Ref 7PHB CHF (EtOH) 30G 10,000 RPM		
Cocoon	Weight (as prepared) (g)	Weight (without CHF) (g)
1	0.168	0.165
2	0.202	0.199
3	0.192	0.189
Average (g)	0.187	0.185
Deviation (g)	0.014	0.015
Deviation (%)	7.7	7.9

Table 4.7: Cocoons weights of cotton-like samples prepared from 7 wt.% P3HB solution in chloroform stab. by ethanol with an addition of 15 wt.% EMERY MC 2192 plasticiser, 30G needles were used

7PHB CHF (EtOH) 30G 10,000 RPM 15 wt.% EMERY MC 2192		
Cocoon	Weight (as prepared) (g)	Weight (without CHF) (g)
1	0.236	0.232
2	0.219	0.217
3	0.203	0.201
4	0.212	0.209
5	0.222	–
6	0.216	0.214
7	0.225	0.221
8	0.227	–
Average (g)	0.218	0.211
Deviation (g)	0.008	0.008
Deviation (%)	3.8	3.5

At the same time, the tables show cocoons weights ‘as prepared‘ and ‘without chloroform‘ in the next column. ‘As prepared‘ means directly after cocoons preparation and ‘without chloroform‘ represents the cocoon weight measured several days afterwards when it was

expected that the whole amount of chloroform would be evaporated. No significant decrease in the weight of the cocoons caused by the evaporation of chloroform was detected. It can be concluded that its content in the fibres was minimal.

4.6 Thermal analysis

The fibres were subjected to thermal analysis. Actual polymer ratios were monitored by TGA, including verification of added plasticiser content. The determined polymer ratios corresponded to the ratios in which they were added to the mixture (4.8). In the case of the addition of plasticiser, slightly lower values were measured, especially at higher concentrations of plasticiser (4.9). The difference in values was a maximum of 3%. The result may be justified due to the limited miscibility of the plasticiser with the polymer and the consequent inability to incorporate the total amount of plasticiser into the fibrous structure during the spinning process.

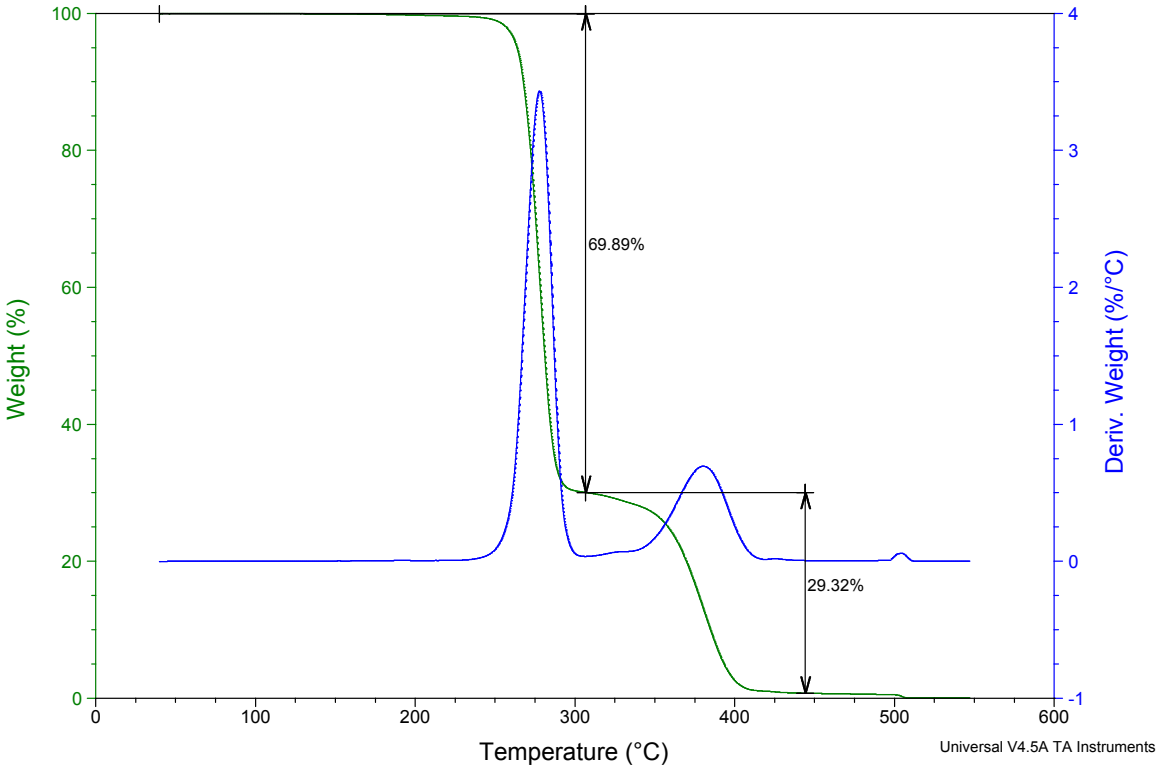

Figure 4.8: TGA curve of fibres prepared from 7 wt.% P3HB solution with an addition of 30 wt.% of PCL

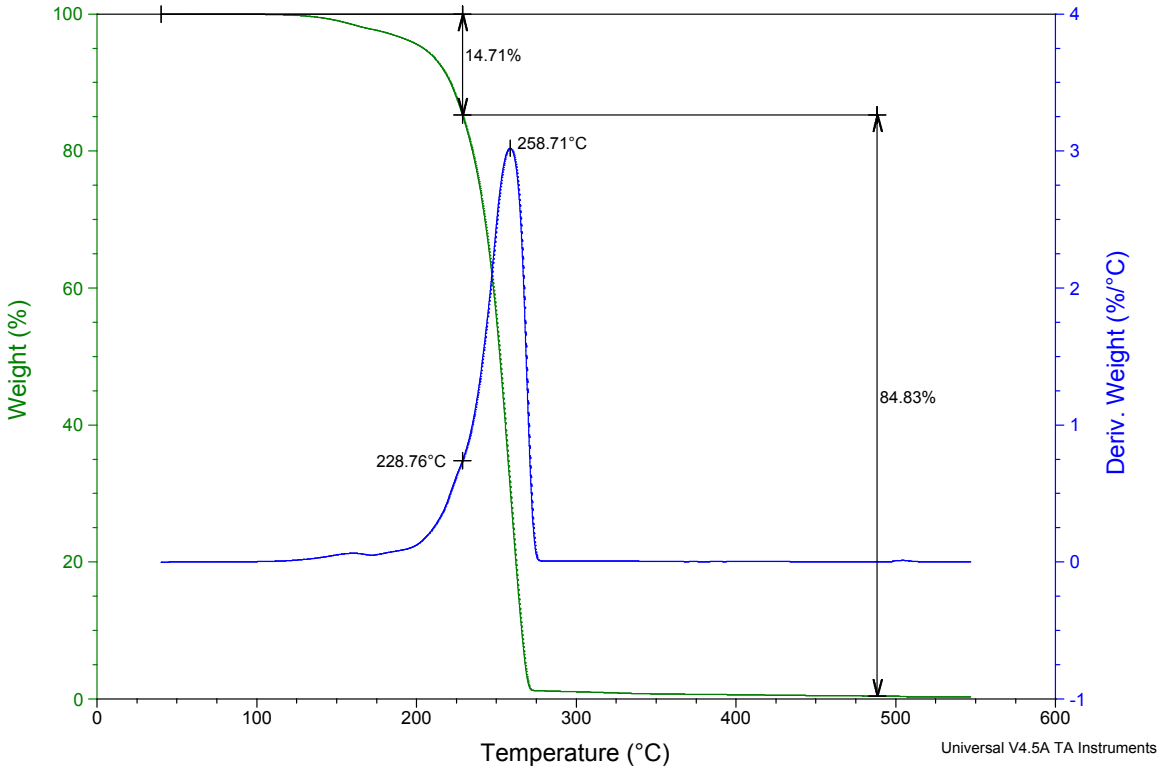

Figure 4.9: TGA curve of fibres prepared from 7 wt.% P3HB solution with an addition of 15 wt.% of A4

DSC analysis monitored the crystallisation of PHB mixtures in the form of solvent casting films in comparison with centrifugal spinning fibres. Enthalpy values of pure PHB foil, PHB fibres and PCL granule were measured and listed in table 4.8. Since PLA is an amorphous polymer was used for this work, enthalpy of PLA was not determined. Based on the DSC analysis, no change in thermal behaviour was observed for the pure PHB sample and the PHB:PLA mixture. The melting enthalpy and thus the crystallinity of PHB corresponded to a relative amount in the mixture with theoretical assumption (4.9).

In contrast, the PHB:PCL mixture showed a difference in the enthalpy of melting and crystallisation of PCL in the fibre and film (see table of measured values - the difference is indicated in bold and the figures 4.10, 4.11). In the case of the solvent casting film, the enthalpy was twice as high as the enthalpy in the fibre sample. The actual PHB and PCL content, which corresponded to the required ratio of 70:30, was verified by TGA. The change in enthalpy is not due to the different polymer ratio in the blend, but that PCL blended with PHB in the fibres appears to form a different crystalline structure with lower crystallinity.

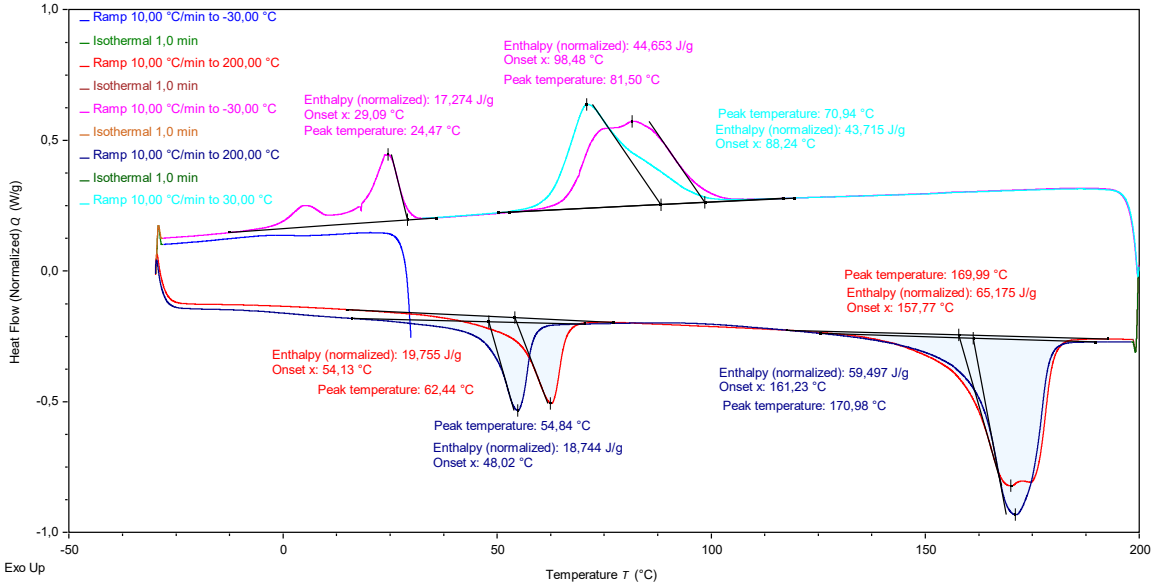

Figure 4.10: DSC analysis of PHB:PCL (70:30) foil with the determined values of enthalpies and peak temperatures

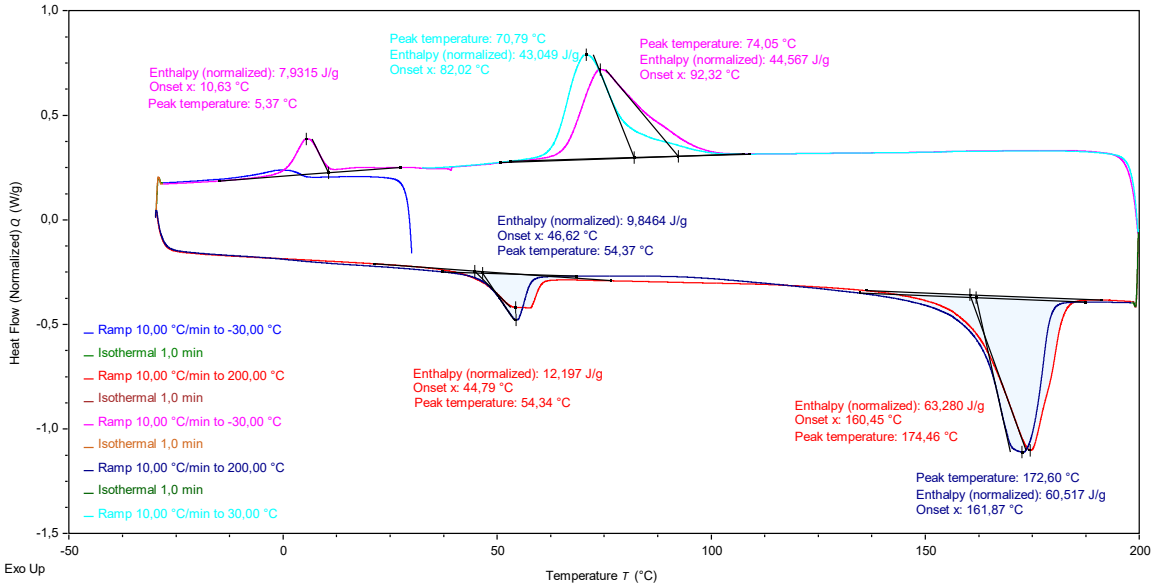

Figure 4.11: DSC analysis of PHB:PCL (70:30) fibres with the determined values of enthalpies and peak temperatures

Table 4.8: Measured enthalpy values of pure PHB foil, PHB fibres, PCL granule and PLA

Sample	**Entalphy of 2nd melting (J/g)**
PHB foil	83.7
PHB fibres	83.8
PCL granule	64.1
PLA	0

Table 4.9: Theoretical determined and measured enthalpy values of pure PHB:PCL (70:30) foil and fibres

	Theoretical assumption	
Sample	**Substances individually**	**Entalphy of 2nd melting (J/g)**
PHB:PCL (70:30)	PHB	58.7
	PCL	**19.2**
	Measured values	
Sample	**Substances individually**	**Entalphy of 2nd melting (J/g)**
PHB:PCL (70:30) foil	PHB	59.5
	PCL	**18.7**
PHB:PCL (70:30) fibres	PHB	60.5
	PCL	**9.8**

4.7 Fibre morphology and fibre diameter

Samples were subjected to SEM and LCSM microscopy. SEM images provide a detailed view of the shape of the fibre, including its surface morphology, and provide at least basic information about the porosity of the sample. A confocal microscope with image analysis was then used to measure fibre diameter.

The fibres of the cotton-like samples were compared in terms of the needle diameter used during the spinning process. The figure shows fibres prepared using 25G, 27G and 30G needles, which correspond to an outer diameter of 0.5, 0.4 and 0.3 mm, respectively. There is no significant difference between the fibres in the SEM. For fibres using a 25G needle, it is possible to observe the orientation of the fibres in one direction. Fibres prepared using a 30 G needle contain fewer clumps compared to fibres prepared by 27 G needles and have a smoother surface.

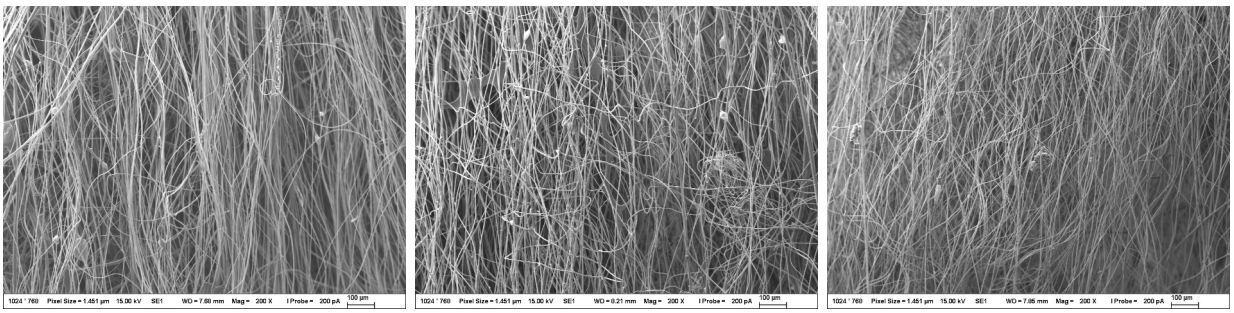

(a) 25G (b) 27G (c) 30G

Figure 4.12: SEM images of fibres prepared using three different types of needle: 25G, 27G and 30G, which corresponds to outer diameter of 0.5, 0.4 and 0.3 mm, respectively

Fibres prepared in the form of a planar substrate from a 7 wt.% solution of P3HB and mixtures in a ratio of 70:30 from P3HB:PLA and P3HB:PCL show a very similar network structure and morphology of the fibre surface. The technology was set for these samples to produce textiles of basis weight 10 g/m^2. The fibres are usually smooth, with no visible pores on their surface. The pore size between the individual fibres was, in all cases, max. 10 µm. The same result was obtained in producing a fabric with a basis weight of 5 g/m^2.

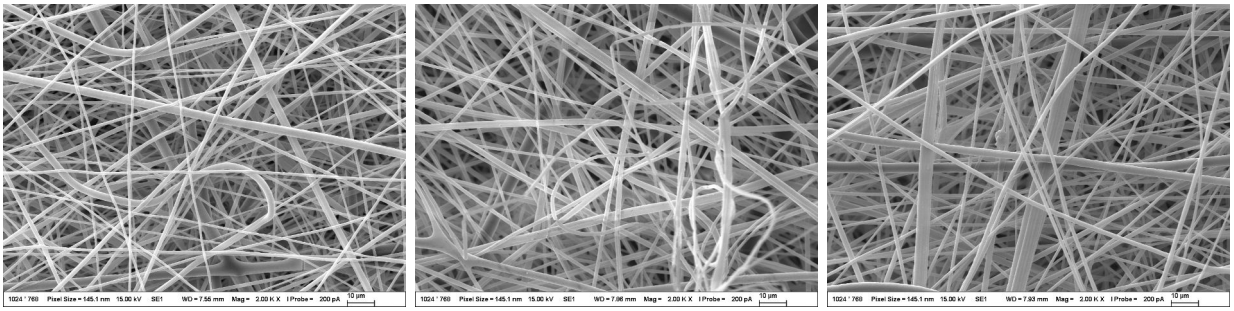

(a) Planar10gsm_PHB (b) Planar10gsm_7PHB_3PLA (c) Planar10gsm_7PHB_3PCL

Figure 4.13: SEM images of fibres prepared as planar substrates on the industrial machine by Nano4Fibers company

There was no marked difference in the results from the SEM in the fibres prepared using needles with different diameters. However, the difference was reflected in the CLSM, where the exact diameters of the individual fibres were determined and compared. It is clear from the table 4.10 and the figure 4.14 that larger diameter needles result in the formation of larger diameter fibres. It is also interesting to note that larger diameter needles have also increased the deviation of the average fibre diameter.

Table 4.10: Diameters of fibres prepared using three different types of needle: 25G, 27G and 30G, which corresponds to outer diameter of 0.5, 0.4 and 0.3 mm, respectively

	25G	**27G**	**30G**
Average (µm)	8.5	4.5	3.8
Deviation (µm)	2.5	1.2	0.6
Deviation (%)	29	25	16

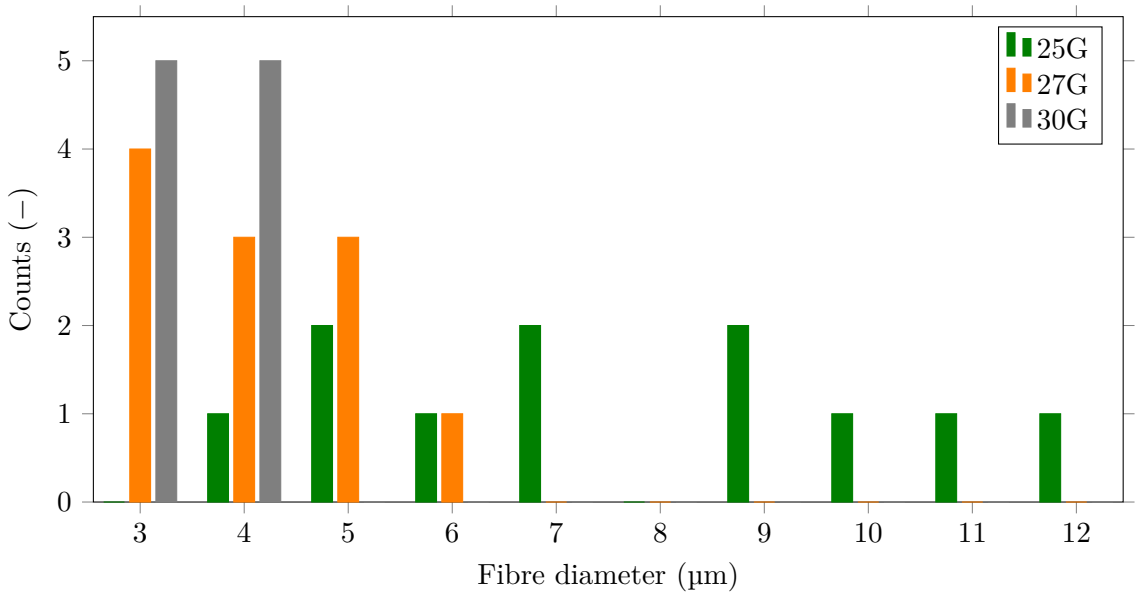

Figure 4.14: Fibre diameters histogram of cotton-like samples prepared using three different types of needles: 25G, 27G and 30G, which corresponds to outer diameter of 0.5, 0.4 and 0.3 mm, respectively

4.8 Mechanical properties

The mechanical properties of wound dressings are an important parameter for their successful use. The fabric itself must have sufficient tensile strength and must be easy to shape without breaking. The values of these parameters are not easily measurable due to the complex structure of microfibers. Likewise, standards with critical values are not yet available. In this work, therefore, the actual materials were compared only with each other and put into context with the process parameters and fiber composition.

A tensile test was chosen to characterise the mechanical properties of the prepared fibrous substrates. Maximum force was converted to stress using the basis weight of the planar samples, length weights for cotton-like samples, respectively. The length weight was determined from the total length of the straightened cocoon and its weight.

The force normalised to a uniform basis weight of 10 GSM was measured for all planar samples, and the value reached approximately 0.75 N. The corresponding tensile stress was

determined to about 17 MPa for all planar samples regardless of the polymer composition of the samples.

For cotton-like samples, the force normalised to a sample weight of 10 mg reaches normalised force values of about 6 N. The values correspond to a tensile strength of about 14 MPa. They are independent of the amount and type of plasticiser used.

Elongation at break of these cotton-like fibrous substrates slightly increased with increasing concentration of plasticiser. The most effective softening effect at 5 wt.% of plasticiser occurred with the use of EMERY MC 2192. However, at a plasticiser content of 15 wt.%, a comparable elongation with the usage of all three types of plasticiser was achieved. The dependence of elongation at break on plasticiser content is shown in figure 4.15.

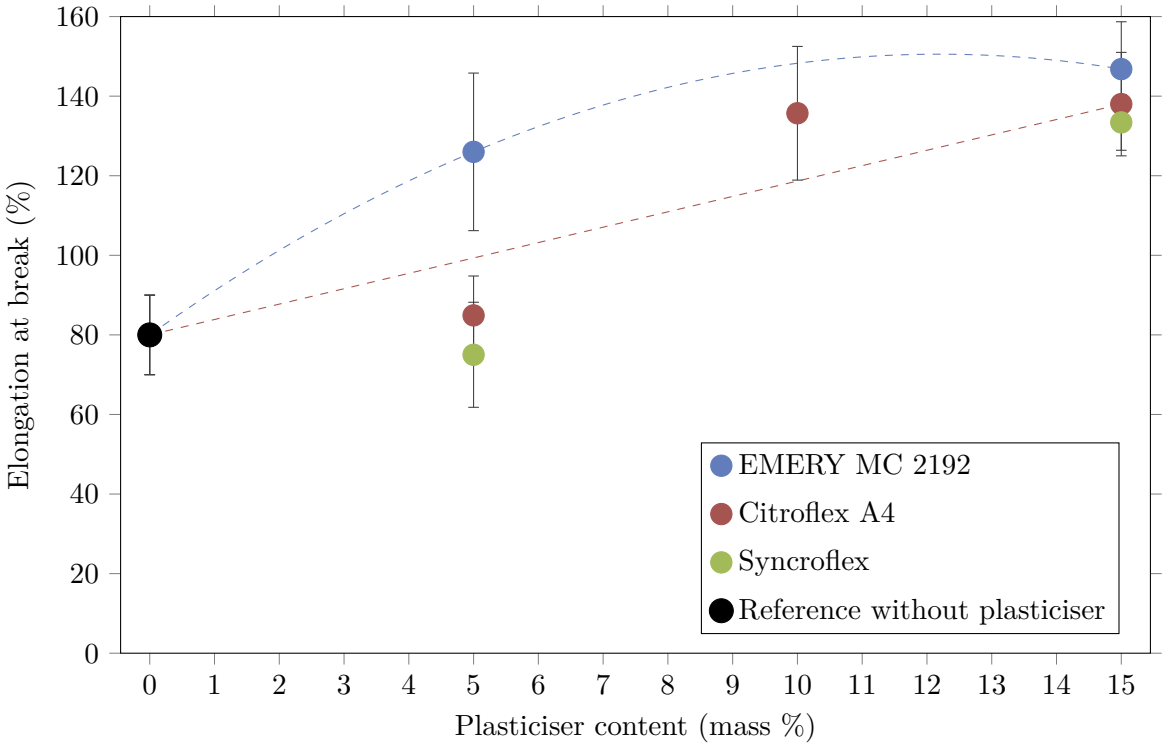

Figure 4.15: Dependence of elongation at break on plasticizer content of 7 wt.% P3HB solution in chloroform stab. by ethanol

4.9 Biological properties

A test of the manipulability of the prepared disk-like samples showed that both forms of fibres could be converted into the form of test samples for biological tests without significant problems. In the case of the cotton-like form of fibres, attention must be paid to the amount (weight respectively) of fibres used to form the disk-like samples to make the samples equivalent. Working with samples is relatively complicated due to the presence of static charge. Most samples are tricky to insert into the wells of the test plate because of their potential to jump out of the wells. However, after the addition of the culture medium, this

problem is eliminated, and the samples can be reliably tested. Lists of samples sent for biological properties tests are presented in the tables 4.11, 4.12.

3T3 fibroblasts seeded on tissue culture plastic were used as a control (it serves as a control of cells condition). Tissue culture plastic is optimized for cell adhesion and growth, so it is normal when values measured on samples are the same or lower.

Table 4.11: List of the first series of samples tested for biological properties

Sample	Sample name	Sample form	Composition
1	Planar10gsm_PHB	planar	PHB
2	Planar10gsm_7PHB_3PLA	planar	PHB:PLA = 70:30
3	Planar10gsm_7PHB_3PCL	planar	PHB:PCL = 70:30
4	Planar5gsm_PHB	planar	PHB
5	Vata27G_PHB	cotton-like	PHB
6	Vata30G_PHB	cotton-like	PHB
7	Vata30G_PHB_10SYNC	cotton-like	P3HB, 10 wt.% SYNC

Table 4.12: List of the second series of samples tested for biological properties

Sample	Sample name	Sample form	Composition
1	Vata30G_PHB	cotton-like	P3HB
2	Planar9gsm_PHB	planar	P3HB
3	Planar15gsm_PCL	planar	PCL
4	LyophorHA	cotton-like	collagen
5	Vata30G_PHB_5MC	cotton-like	P3HB, 5 wt.% EMERY MC 2192
6	Vata30G_PHB_15MC	cotton-like	P3HB, 15 wt.% EMERY MC 2192
7	Vata30G_PHB_5A4	cotton-like	P3HB, 5 wt.% A4
8	Vata30G_PHB_15A4	cotton-like	P3HB, 15 wt.% A4
9	Vata30G_PHB_5SYNC	cotton-like	P3HB, 5 wt.% SYNC
10	Vata30G_PHB_15SYNC	cotton-like	P3HB, 15 wt.% SYNC
11	3D Biotek Insert PS	3D-printed	polystyrene
12	3D Biotek Insert PCL	3D-printed	PCL
13	Planar13gsm_PLA	planar	PLA (amorphous)

During the sterilization process or transport to the laboratory providing tests of biological properties, the prepared disk-like samples with number 13 were shrunk, which is visible in the figure 4.16. Therefore, Planar13gsm_PLA sample was excluded from testing the second series of samples.

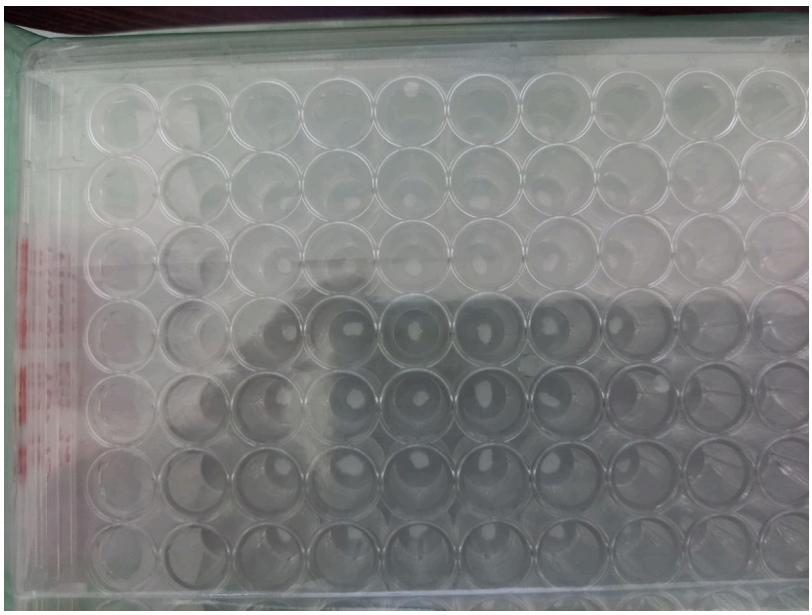

Figure 4.16: Planar13gsm_PLA samples that were damaged during transport

The scaffolds were pre-wet by culture medium at 37 °C before seeding. The scaffolds 1-4 in the first series and scaffolds 2 and 3 in the second series were hydrophobic. The rest of the scaffolds was hydrophilic and soaked immediately after putting the scaffolds on the culture media on the bottom of the well plate. After resting the scaffolds in the incubator, most of the scaffold were soaked by the medium. However, still, there were some small non-wet areas. While controlling the bottom of the well underneath the hydrophobic scaffolds, an almost confluent layer of the cell was observed beneath the scaffolds. The rest of the groups had cells only on the edges of the bottom of the well. This is caused by mentioned strong hydrophobicity. The result is that the droplet with the cells slipped underneath the scaffold on the bottom of the well.

The non-homogeneity of the samples probably resulted in a diversity of values measured in MTS analysis and DNA quantification and was also visible in confocal microscopy visualization. The non-homogeneity is visible from a photography of a well plate with a solution of MTS after incubation with cell-seeded scaffolds (4.17). The product of metabolized cells is purple formazan. A darker solution means more metabolically active cells. The groups are arranged in the columns; lower light samples are control scaffolds without cells.

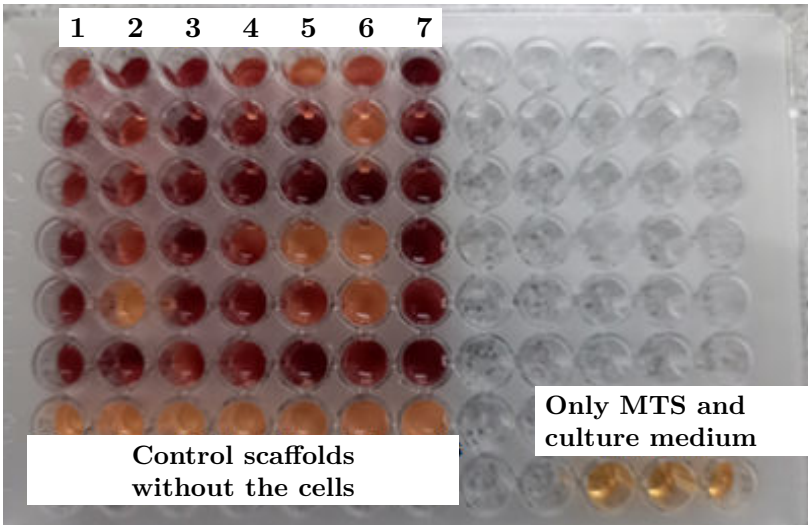

Figure 4.17: Photography of well plate with MTS solution after 2 hours incubation with cell-seeded scaffolds. Darker color means bigger number of metabolically active cells

As was mentioned above, the measurement of metabolic activity was affected by the non-homogeneity of the samples. Figure 4.18 shows the measured values without the marginal values that were left out. Metabolic activity was comparable on all scaffolds on day 1 and 3. The only exception was that metabolic activity was higher on sample 7 than sample 1 on day 1. On day 7, metabolic activity increased on samples 1, 2, 3, 4 and 7, respectively. On the other hand, absorbance decreased on samples 5 and 6, where the lowest values were measured. The highest values were obtained for cells cultured on culture plastic, which is ordinary considering that it is optimised for cell growth. Also, the effectiveness of the seeding is 100% on the bottom of the well plate.

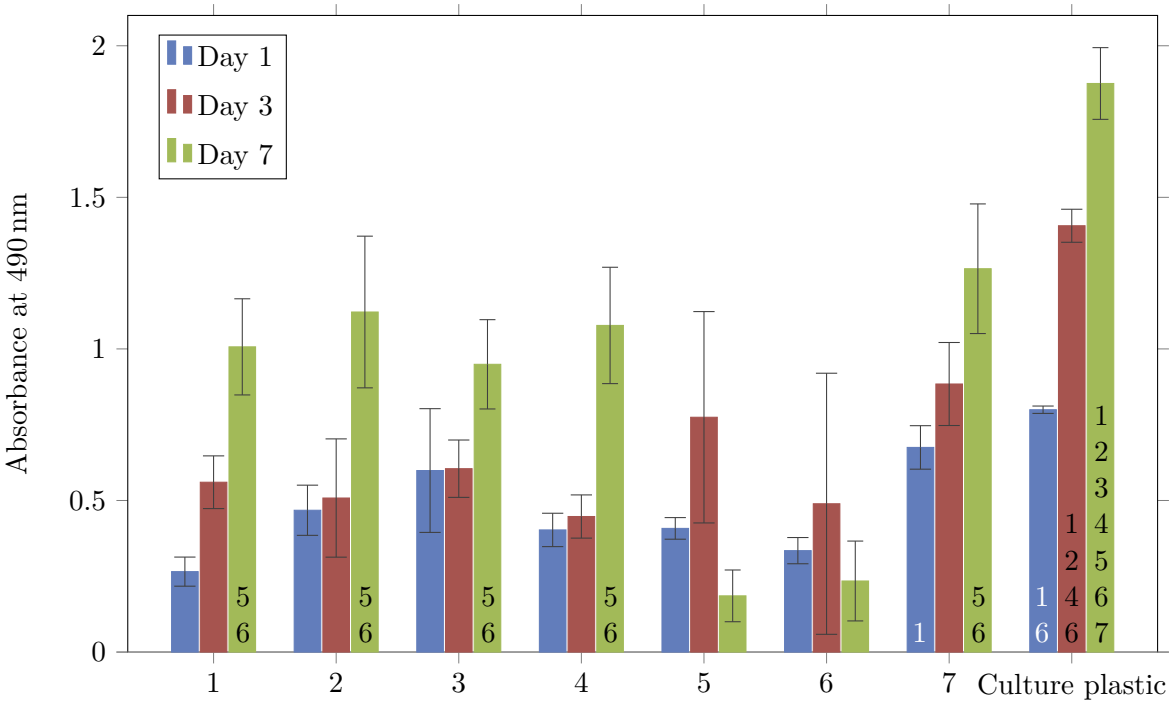

Figure 4.18: Metabolic activity of the cells cultured on nanofibrous scaffolds from the first series measured using MTS analysis. 3T3 fibroblasts cultured on tissue culture plastic were used as a control. Measured values were non-homogenous, which resulted in high standard deviations (A). Graph B did not contain margin values. Numbers above the columns sign statistical significance, white numbers - $p < 0.05$, black numbers – $p < 0.001$

The cell proliferation was measured using DNA quantification (Fig 4.19. The best cell adhesion was detected on sample 3, where the highest cell number was measured. Cell number was higher on sample 2 compared to samples 1 and 6 on day 1. On day 3, cell numbers were comparable on all samples. While cell numbers increased on samples 1, 2, 3, 4, and 7, respectively, a decrease was detected on sample 5 and 6. Nevertheless, the only statistical difference was detected on sample 7, where cell number was higher compared to sample 5 and 6.

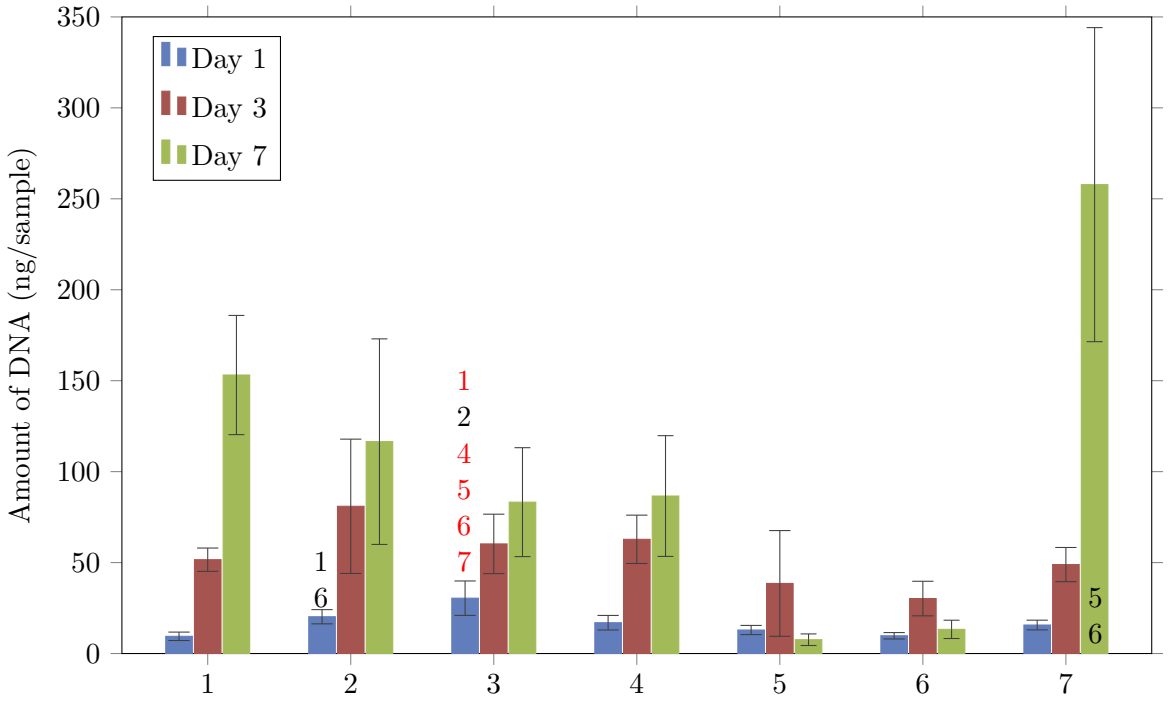

Figure 4.19: Cell proliferation of the samples from the first series was measured using DNA quantification. Numbers above the columns sign statistical significance, black numbers - $p<0.05$, red numbers – $p<0.001$

The results from the MTS assay of the samples from the first series showed the positive impact of plasticizer. Based on the results, it was decided that the second series of samples tested on biological properties will concentrate on the addition of plasticizers. The results from the metabolic activity test of the second series of samples are shown in figure 4.20.

The highest metabolic activity was measured on culture plastic and then on samples 13 and 4 on day 1. The absorbance was comparable to other samples. On day 3, the highest metabolic activity was detected on culture plastic and then on sample 7. The lowest metabolic activity was measured on samples 2, 3 and 5. On day 7, the highest absorbance was measured on culture plastic, followed by samples 11, 13, and 7. On the other hand, the lowest metabolic activity was detected in sample 2.

To summarise the results from metabolic activity measurement, the best cell adhesion was detected on sample 4 (Lyophor). The absorbance was comparable among the fibrous scaffolds. In the following days, the highest metabolic activity was measured on sample 7 (Vata30G_PHB_5A4). On day 7, it was higher than commercially available samples 4 and 12 and comparable to 3D Biotek Insert PS. The lowest metabolic activity was measured on samples 2 and 3, the planar samples and 5 (Vata30G_PHB_5MC). Sample 13 should not be compared with other samples, as it was just dipped in the culture medium of the cells cultured on the culture plastic. The result shows that the sample is not cytotoxic.

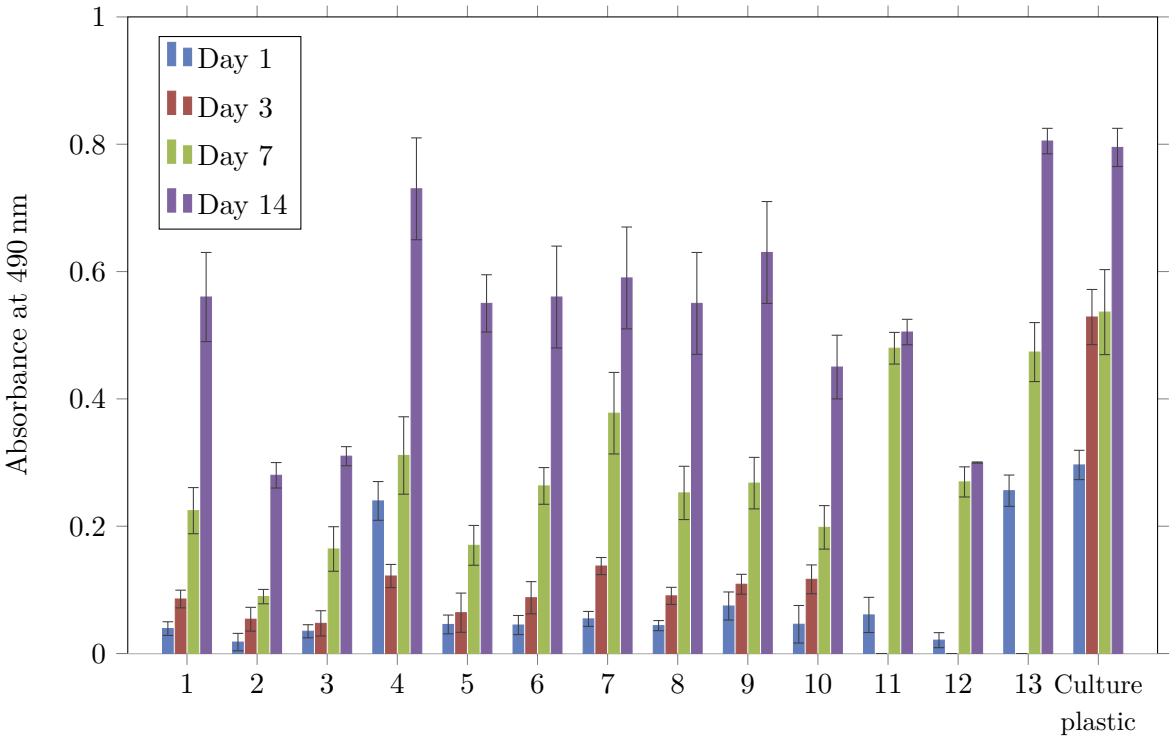

Figure 4.20: Metabolic activity of the cells cultured on nanofibrous scaffolds from the second series measured using MTS analysis. 3T3 fibroblasts cultured on tissue culture plastic were used as a control.

The cell proliferation was measured using DNA quantification (Fig 4.21). The analysis did not show many differences between the samples as the measured values were not homogenous. The adhesion was comparable on all fibrous samples and, except sample 1, was similar to culture plastic. On day 3, the highest cell number was detected on sample 4 and 6. On day 7, the lowest cell number was detected on sample 3. The other samples were comparable to commercially available samples and culture plastic.

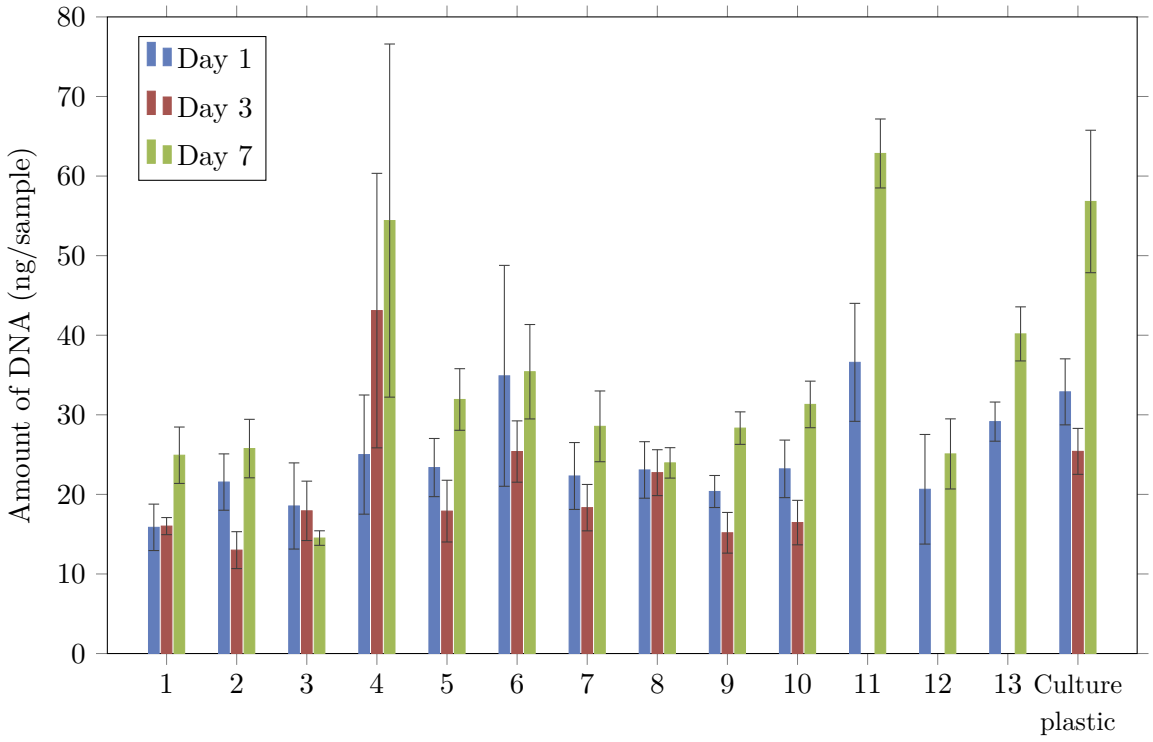

Figure 4.21: Cell proliferation of the samples from the second series was measured using DNA quantification.

Cell distribution on scaffolds was visualized using confocal microscopy (Fig. 4.22). The cell nuclei were stained using propidium iodide and intracellular membranes using DiOC6(3) on days 1 and 7. The cells were well adhered to all the samples. The distribution of the cells on the scaffolds was nonhomogeneous. There were significant differences in the cell amount between individual samples in one group. The depth of cell penetration was between 50 – 70 µm (Fig. 4.23). Interestingly, the penetration was comparable for both planar and fluffy scaffolds. Among the fibrous scaffolds, the most infiltrated by the cells was sample 8; it was 110 µm on day 7. The penetration depth was comparable with the collagen foam Lyophor. It is difficult to compare the penetration of cells in fibrous scaffolds and the commercial 3D Biotec inserts, as the inserts are 3D printed and have entirely different morphology.

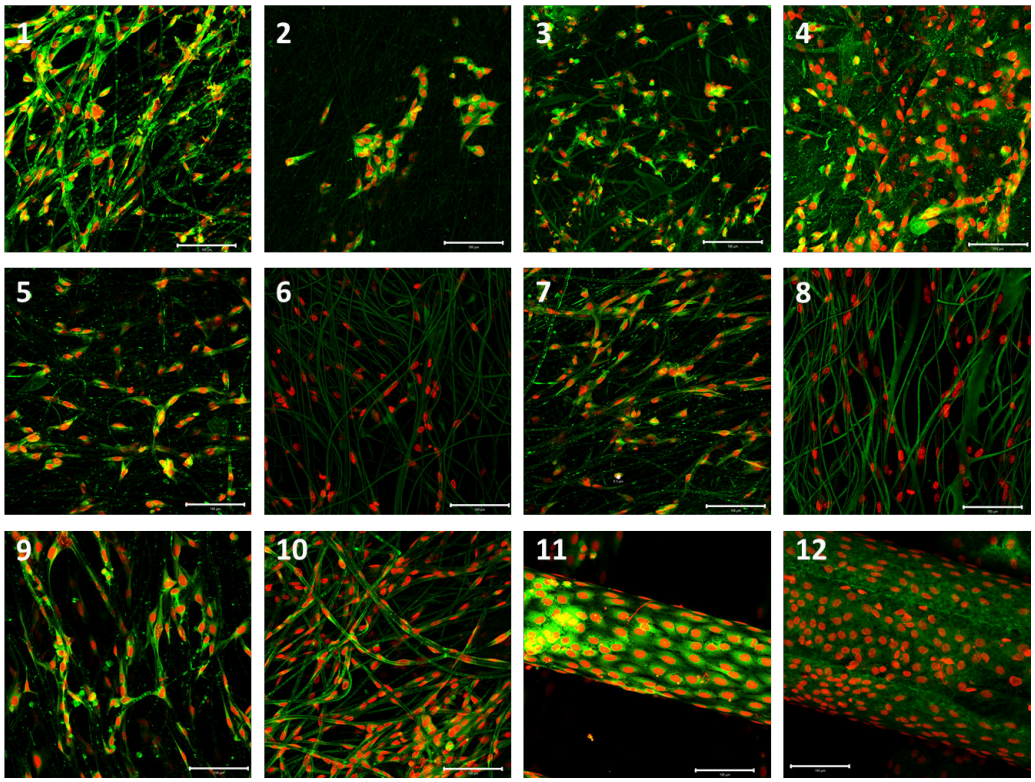

Figure 4.22: Cell distribution on nanofibrous scaffolds on day 7. Cell nuclei were stained using propidium iodide (red color), intracellular membranes using $DiOC_6(3)$ (green color). Magnification 200×, scale bar 100 µm

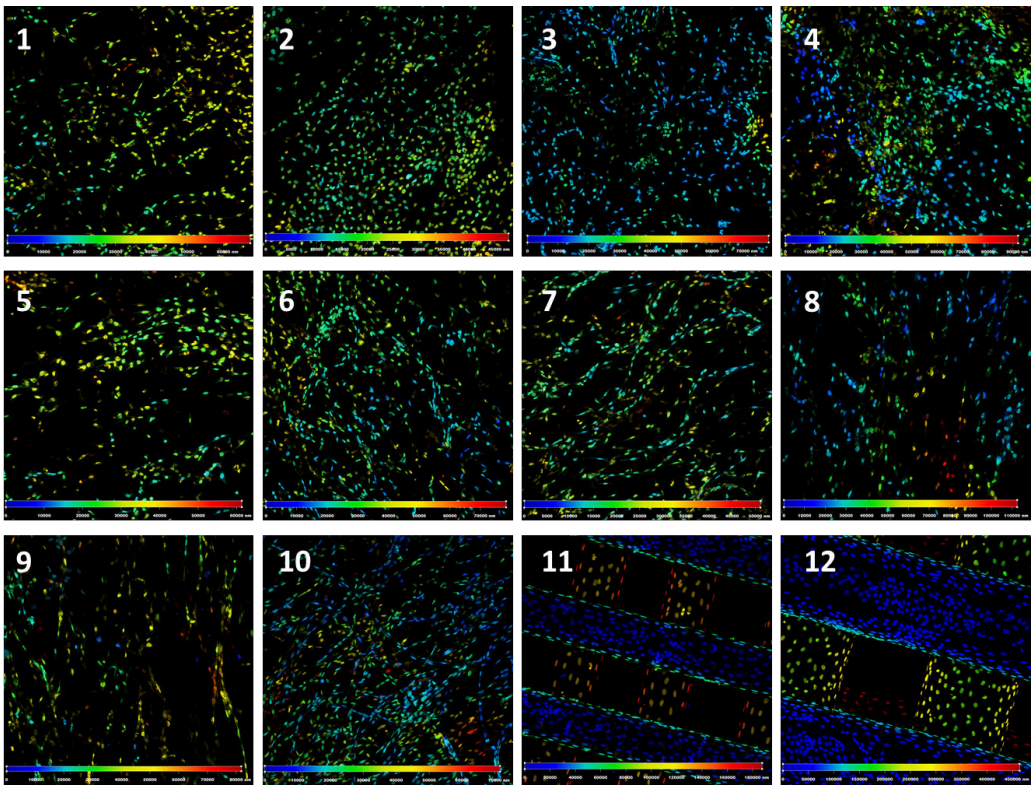

Figure 4.23: Cell penetration into the fibrous scaffolds on day 7. Color-coded projection of cell nuclei stained using propidium iodide. Different colors were denoted to cell nuclei in different depth of the scaffold. The color scale is at the lower edge of the figures. Magnification 100 ×

5 Conclusion

The work dealt with developing microfiber substrates based on P3HB produced by centrifugal spinning for medical applications. Therefore, a substantial part of the practical work was devoted to getting acquainted with this technology and process parameters affecting the final product - microfiber fabric. The key parameters of this process are the viscosity of the solution controlled by the concentration of the polymer solution and the molecular weight, the method of dosing into the rotary spinneret, the rotation speed of the spinning nozzle and the diameter of the spinning nozzles or needles. Subsequently, these parameters were optimized to produce fibres from solutions of P3HB in chloroform. Therefore, some of the results describe the significant effect of chloroform stabilization on the resulting properties of the solution and the spinning process and the issue of the effect of molecular weight on the spinning process. The tests were carried out on a commercial laboratory spinning machine at FEEC BUT, which was subsequently equipped with a syringe pump and a nozzle for continuous fibre production due to inappropriate discontinuous dosing of the solution. Thus, it was possible to control the dosing process better and create enough material for biological tests and tests of mechanical properties. This process on a laboratory machine produced samples in the form of cotton-like bundles. The diameter of the fibres in the range from 3 to 12 µm depending on the selected diameter of the spinning needle was determined by microscopy and image analysis. At the same time, the optimized solutions were tested in the partner company NANO4FIBERS s.r.o on an industrial system, which produced planar samples with a basis weight of 5, 10 and 15 g/m^2 for this work. The diameter of the fibres thus prepared was in the range of 0.5–2 µm.

According to the research, P3HB alone is not very suitable for this application due to the relatively small polar component of the surface tension and thus the low wettability by aqueous solutions and due to the embrittlement of the fibres over time. One of the proposed solutions was to mix other polymeric biocompatible polymers into the P3HB solution. PLA, PCL and PEG were selected. Based on experience with blends of these polymers in the melt, a mixing ratio of P3HB to an auxiliary polymer of 70:30 was determined and fixed as fixed for this work. The P3HB:PEG solution failed to spin, the P3HB:PLA and P3HB:PCL blends were spun successfully, and the resulting fibres were morphologically similar to pure P3HB fibres.

A plasticizer additive has proven to be a second method suitable for controlling the properties of the fibres. In the work, 3 plasticizers of different chemical structures were tested. These plasticizers were added to the P3HB solution in three concentrations relative to the polymer content (5, 10 and 15%). All solutions were successfully spun into high-quality fibrous structures. After optimizing the process parameters, it was also possible to consider the fibre preparation process as reproducible.

The properties of fibrous structures were assessed in terms of thermal properties. The percentage of individual material components in the fibre was checked by TGA. Within

the error of about 10%, it was possible to prove the same composition of fibres compared to the solution and thus exclude the separation of some components during the spinning process. The crystallization behaviour of the polymer fibre was evaluated from DSC, especially with regard to the achieved crystallinity. The melting enthalpy of P3HB in the mixtures corresponded to its percentage content. However, half the relative enthalpy of melting of PCL was observed in the PHB: PCL fibres compared to pure PCL as well as to the solvent-casted film of the same material composition. It is possible that PCL does not achieve such crystallinity in the process of a dynamic spinning process as in the case of long-term solvent evaporation in solvent casting film preparation. In order to compare the mechanical properties of the prepared samples, a tensile test was performed, and the measured parameters were normalized with respect to the weight of the sample. The measured force was then related to the theoretical cross-section of the polymeric material itself without air gaps. The maximum tensile stress was thus comparable even between planar and cotton-like samples. The composition of the polymer mixture did not fundamentally affect the tensile strength but allows to control of the maximum deformation effectively. According to the assumption, the plasticizer increased the elongation at break from 80 % to 140 %. The addition of PLA to PHB slightly increases the strength at the expense of ductility. Unfortunately, the addition of PCL to the PHB could not be assessed due to the irreversible loss of the measured data of this sample.

An important characteristic of the prepared samples were tests of metabolic activity and growth of 3T3 fibroblasts cells performed externally at the Department of Tissue Engineering, Institute of Experimental Medicine of CAS. From the results of 2 series it can be concluded that all prepared materials are biocompatible and non-toxic for selected cells. The metabolic activity of the cells and their proliferation from the first series of tests on cotton-like substrates from pure P3HB was significantly lower on day 7 than when using 10 % Syncroflex plasticizer. However, this was not confirmed in the second test, which took place for 14 days, where the results of the metabolic activity of the cells after 14 days of culture were comparable, taking into account the statistical error with all the softened substrates used. In contrast to the best tested commercial substrates, P3HB-based samples achieve approximately 80 percent of the metabolic activity values, indicating suitable properties for the intended applications. Unsoftened P3HB and PCL planar substrates show comparable results but significantly lower compared to softened ones.

In terms of the effect of the morphology of the tested P3HB samples, it can be stated that the metabolic activity of cotton-like substrates is twice as high as in planar samples. The results of proliferation on day 14 were not yet available at the time of the diploma thesis. In the case of PCL planar substrate and commercial 3D printed substrate, comparable results were obtained in the metabolic activity of cells and in their proliferation as well.

The results show that mixtures of P3HB and PCL and PLA optionally softened with a suitable plasticizer can be used in the intended application of a wound cover or 3D substrate for cell tests. However, research in this area is at the very beginning, and this diploma thesis only maps the real technical possibilities of centrifugal spinning of this biomaterial in the mentioned mixtures. Work on this topic will continue in a follow-up project and will focus on the synergy of the effect of plasticizer and added biopolymer material to P3HB. The big future challenge is to map the spinnability and biocompatibility in connection with the used P3HB extraction method, which affects both the molecular weight and possible residues of cell walls and other substances from the fermentation process.

Bibliography

[1] Loordhuswamy, A. M., Krishnaswamy, V. R., Korrapati, P. S., Thinakaran, S. and Rengaswami, G. D. V. Fabrication of highly aligned fibrous scaffolds for tissue regeneration by centrifugal spinning technology. *Materials Science and Engineering: C*. 2014, vol. 42, p. 799–807. DOI: https://doi.org/10.1016/j.msec.2014.06.011. ISSN 0928-4931. Available at: https://www.sciencedirect.com/science/article/pii/S0928493114003737.

[2] Li, C., Huang, Y., Li, R., Wang, Y., Xiang, X. et al. Fabrication and properties of carboxymethyl chitosan/polyethylene oxide composite nonwoven mats by centrifugal spinning. *Carbohydrate Polymers*. 2021, vol. 251, p. 117037. DOI: https://doi.org/10.1016/j.carbpol.2020.117037. ISSN 0144-8617. Available at: https://www.sciencedirect.com/science/article/pii/S0144861720312108.

[3] Shishatskaya, E., Nikolaeva, E., Vinogradova, O. and Volova, T. Experimental wound dressings of degradable PHA for skin defect repair. *Journal of Materials Science: Materials in Medicine*. 2016, vol. 27, p. 1–16.

[4] *Understanding Microfiber's Role in Infection Prevention* [online]. Infection Control Today, November 2008 [cit. 2021-05-10]. Available at: https://www.infectioncontroltoday.com/view/understanding-microfibers-role-infection-prevention.

[5] Liu, J., Yang, Y., Ding, J., Zhu, B. and Gao, W. Microfibers: a preliminary discussion on their definition and sources. *Environmental Science and Pollution Research*. october 2019, vol. 26. DOI: 10.1007/s11356-019-06265-w.

[6] Matica, A., Aachmann, Tøndervik, Sletta, H. and Ostafe. Chitosan as a Wound Dressing Starting Material: Antimicrobial Properties and Mode of Action. *International Journal of Molecular Sciences*. november 2019, vol. 20, p. 5889. DOI: 10.3390/ijms20235889.

[7] Mukhopadhyay, S. and Ramakrishnan, G. Microfibres. *Textile Progress*. Taylor & Francis. 2008, vol. 40, no. 1, p. 1–86. DOI: 10.1080/00405160801942585. Available at: https://doi.org/10.1080/00405160801942585.

[8] Kusindarta, D. and Wihadmadyatami, H. The Role of Extracellular Matrix in Tissue Regeneration. In:. June 2018. DOI: 10.5772/intechopen.75728. ISBN 978-1-78923-260-8.

[9] Hess, E., Madayag, A., Hearing, M. and Baker, D. A. Chapter 16 - Glial Dysregulation in Addiction. In: Torregrossa, M., ed. *Neural Mechanisms of*

Addiction. Academic Press, 2019, p. 237–246. DOI: https://doi.org/10.1016/B978-0-12-812202-0.00016-6. ISBN 978-0-12-812202-0. Available at: https://www.sciencedirect.com/science/article/pii/B9780128122020000166.

[10] Hutten, I. M. CHAPTER 5 - Processes for Nonwoven Filter Media. In: Hutten, I. M., ed. *Handbook of Nonwoven Filter Media*. Oxford: Butterworth-Heinemann, 2007, p. 195–244. DOI: https://doi.org/10.1016/B978-185617441-1/50020-2. ISBN 978-1-85617-441-1. Available at: https://www.sciencedirect.com/science/article/pii/B9781856174411500202.

[11] Geus, H.-G. 5 - Developments in manufacturing techniques for technical nonwovens. In: Kellie, G., ed. *Advances in Technical Nonwovens*. Woodhead Publishing, 2016, p. 133–153. Woodhead Publishing Series in Textiles. DOI: https://doi.org/10.1016/B978-0-08-100575-0.00005-X. ISBN 978-0-08-100575-0. Available at: https://www.sciencedirect.com/science/article/pii/B978008100575000005X.

[12] Hagewood, J. 3 - Technologies for the manufacture of synthetic polymer fibers. In: Zhang, D., ed. *Advances in Filament Yarn Spinning of Textiles and Polymers*. Woodhead Publishing, 2014, p. 48–71. DOI: https://doi.org/10.1533/9780857099174.1.48. ISBN 978-0-85709-499-5. Available at: https://www.sciencedirect.com/science/article/pii/B9780857094995500039.

[13] Jose Varghese, R., Mamour Sakho, E. hadji, Parani, S., Thomas, S., Oluwafemi, O. S. et al. Chapter 3 - Introduction to nanomaterials: synthesis and applications. In: Thomas, S., Sakho, E. H. M., Kalarikkal, N., Oluwafemi, S. O. and Wu, J., ed. *Nanomaterials for Solar Cell Applications*. Elsevier, 2019, p. 75–95. DOI: https://doi.org/10.1016/B978-0-12-813337-8.00003-5. ISBN 978-0-12-813337-8. Available at: https://www.sciencedirect.com/science/article/pii/B9780128133378000035.

[14] Zheng, Y. 3 - Fabrication on bioinspired surfaces. In: Zheng, Y., ed. *Bioinspired Design of Materials Surfaces*. Elsevier, 2019, p. 99–146. Materials Today. DOI: https://doi.org/10.1016/B978-0-12-814843-3.00003-X. ISBN 978-0-12-814843-3. Available at: https://www.sciencedirect.com/science/article/pii/B978012814843300003X.

[15] Sabantina, L. Chapter 11 - Nanocarbons-based textiles for flexible energy storage. In: Ehrmann, A., Nguyen, T. A. and Nguyen Tri, P., ed. *Nanosensors and Nanodevices for Smart Multifunctional Textiles*. Elsevier, 2021, p. 163–188. Micro and Nano Technologies. DOI: https://doi.org/10.1016/B978-0-12-820777-2.00011-X. ISBN 978-0-12-820777-2. Available at: https://www.sciencedirect.com/science/article/pii/B978012820777200011X.

[16] Gopanna, A., Rajan, K. P., Thomas, S. P. and Chavali, M. Chapter 6 - Polyethylene and polypropylene matrix composites for biomedical applications. In: Grumezescu, V. and Grumezescu, A. M., ed. *Materials for Biomedical Engineering*. Elsevier, 2019, p. 175–216. DOI: https://doi.org/10.1016/B978-0-12-816874-5.00006-2. ISBN 978-0-12-816874-5.

Available at:
https://www.sciencedirect.com/science/article/pii/B9780128168745000062.

[17] Zhang, L., Aboagye, A., Kelkar, A., Lai, C. and Fong, H. A review: carbon nanofibers from electrospun polyacrylonitrile and their applications. *Journal of Materials Science*. 2013, vol. 49, p. 463–480.

[18] Radacsi, N. and Nuansing, W. Chapter 7 - Fabrication of 3D and 4D polymer micro- and nanostructures based on electrospinning. In: Sadasivuni, K. K., Deshmukh, K. and Almaadeed, M. A., ed. *3D and 4D Printing of Polymer Nanocomposite Materials*. Elsevier, 2020, p. 191–229. DOI: https://doi.org/10.1016/B978-0-12-816805-9.00007-7. ISBN 978-0-12-816805-9. Available at:
https://www.sciencedirect.com/science/article/pii/B9780128168059000077.

[19] Obregon, N., Agubra, V., Pokhrel, M., Campos, H., Flores, D. et al. Effect of Polymer Concentration, Rotational Speed, and Solvent Mixture on Fiber Formation Using Forcespinning®. *Fibers*. june 2016, vol. 4, p. 20. DOI: 10.3390/fib4020020.

[20] Gramley, K. *FibeRio Announces Release of Cyclone L-1000: Enables Forcespinning™ Nanofibers* [online]. CISION PRWeb, November 2010 [cit. 2021-05-10]. Available at: https://www.prweb.com/releases/2010/11/prweb4740564.htm.

[21] Zhao, Y., Qiu, Y., Wang, H., Yu, C., Jin, S. et al. Preparation of Nanofibers with Renewable Polymers and Their Application in Wound Dressing. *International Journal of Polymer Science*. march 2016, vol. 2016, p. 1–17. DOI: 10.1155/2016/4672839.

[22] Zhang, Z. and Sun, J. Research on the development of the centrifugal spinning. *MATEC Web of Conferences*. january 2017, vol. 95, p. 07003. DOI: 10.1051/matecconf/20179507003.

[23] Correia, D. M., Ribeiro, C., Ferreira, J. C., Botelho, G., Ribelles, J. L. G. et al. Influence of electrospinning parameters on poly(hydroxybutyrate) electrospun membranes fiber size and distribution. *Polymer Engineering & Science*. 2014, vol. 54, no. 7, p. 1608–1617. DOI: https://doi.org/10.1002/pen.23704. Available at:
https://onlinelibrary.wiley.com/doi/abs/10.1002/pen.23704.

[24] Acevedo, F., Villegas, P., Urtuvia, V., Hermosilla, J., Navia, R. et al. Bacterial polyhydroxybutyrate for electrospun fiber production. *International Journal of Biological Macromolecules*. 2018, vol. 106, p. 692–697. DOI: https://doi.org/10.1016/j.ijbiomac.2017.08.066. ISSN 0141-8130. Available at:
https://www.sciencedirect.com/science/article/pii/S0141813017314113.

[25] Pachence, J. M., Bohrer, M. P. and Kohn, J. Chapter Twenty-Three - Biodegradable Polymers. In: Lanza, R., Langer, R. and Vacanti, J., ed. *Principles of Tissue Engineering (Third Edition)*. Third Editionth ed. Burlington: Academic Press, 2007, p. 323–339. DOI: https://doi.org/10.1016/B978-012370615-7/50027-5. ISBN 978-0-12-370615-7. Available at:
https://www.sciencedirect.com/science/article/pii/B9780123706157500275.

[26] Ninan, N., Mohan Bhagyaraj, S. and Francis, E. *Natural Polymers, Biopolymers, Biomaterials, and Their Composites, Blends, and IPNs*. July 2012. ISBN 9781926895161.

[27] Ekwueme, E., Patel, J., Freeman, J. and Danti, S. 17 - Applications of bioresorbable polymers in the skeletal systems (cartilages, tendons, bones). In: Perale, G. and Hilborn, J., ed. *Bioresorbable Polymers for Biomedical Applications*. Woodhead Publishing, 2017, p. 391–422. DOI: https://doi.org/10.1016/B978-0-08-100262-9.00017-3. ISBN 978-0-08-100262-9. Available at: https://www.sciencedirect.com/science/article/pii/B9780081002629000173.

[28] Sinha Ray, S. 5 - Environmentally friendly polymer nanocomposites using polymer matrices from renewable sources. In: Sinha Ray, S., ed. *Environmentally Friendly Polymer Nanocomposites*. Woodhead Publishing, 2013, p. 89–156. Woodhead Publishing Series in Composites Science and Engineering. DOI: https://doi.org/10.1533/9780857097828.1.89. ISBN 978-0-85709-777-4. Available at: https://www.sciencedirect.com/science/article/pii/B978085709777450005X.

[29] HILL, R. G. 10 - Biomedical polymers. In: Hench, L. L. and Jones, J. R., ed. *Biomaterials, Artificial Organs and Tissue Engineering*. Woodhead Publishing, 2005, p. 97–106. Woodhead Publishing Series in Biomaterials. DOI: https://doi.org/10.1533/9781845690861.2.97. ISBN 978-1-85573-737-2. Available at: https://www.sciencedirect.com/science/article/pii/B9781855737372500109.

[30] Polotti, G. Chapter Eight - Perspectives from industry. In: Moscatelli, D. and Sponchioni, M., ed. *Advances in Polymer Reaction Engineering*. Academic Press, 2020, vol. 56, no. 1, p. 259–330. Advances in Chemical Engineering. DOI: https://doi.org/10.1016/bs.ache.2020.07.003. ISSN 0065-2377. Available at: https://www.sciencedirect.com/science/article/pii/S0065237720300235.

[31] Rudnik, E. 13 - Compostable Polymer Properties and Packaging Applications. In: Ebnesajjad, S., ed. *Plastic Films in Food Packaging*. Oxford: William Andrew Publishing, 2013, p. 217–248. Plastics Design Library. DOI: https://doi.org/10.1016/B978-1-4557-3112-1.00013-2. ISBN 978-1-4557-3112-1. Available at: https://www.sciencedirect.com/science/article/pii/B9781455731121000132.

[32] Lizarraga, L., Thomas, C., Cadiz Miranda, J. I. and Roy, I. Tissue Engineering: Polyhydroxyalkanoate-Based Materials and Composites. In:. December 2018. ISBN 9781351019415.

[33] Chen, G.-Q. and Wu, Q. The application of polyhydroxyalkanoates as tissue engineering materials. *Biomaterials*. 2005, vol. 26, no. 33, p. 6565–6578. DOI: https://doi.org/10.1016/j.biomaterials.2005.04.036. ISSN 0142-9612. Available at: https://www.sciencedirect.com/science/article/pii/S0142961205003510.

[34] Porrett, P. *The Surgical Review: An Integrated Basic and Clinical Science Study Guide*. Lippincott Williams & Wilkins, 2010. ISBN 9781451122138. Available at: https://books.google.cz/books?id=b5vumG_1-gIC.

[35] Ogedegbe, H. O. An Overview of Hemostasis. *Laboratory Medicine*. december 2002, vol. 33, no. 12, p. 948–953. DOI: 10.1309/50UQ-GUPF-W6XW-1X7B. ISSN 0007-5027. Available at: https://doi.org/10.1309/50UQ-GUPF-W6XW-1X7B.

[36] Sherratt, J. A. and Murray, J. D. Models of Epidermal Wound Healing. *Proceedings: Biological Sciences*. The Royal Society. 1990, vol. 241, no. 1300, p. 29–36. ISSN 09628452. Available at: http://www.jstor.org/stable/76724.

[37] *Influx of WBC* [online]. Embibe App [cit. 2021-05-10]. Available at: https://www.embibe.com/study/influx-of-wbc-concept.

[38] Nunez, K. *What Is Wound Debridement and When Is It Necessary?* [online]. Healthline, February 2019 [cit. 2021-05-01]. Available at: https://www.healthline.com/health/debridement.

[39] Peng, Y., Ma, Y., Bao, Y., Liu, Z., Chen, L. et al. Electrospun PLGA/SF/artemisinin composite nanofibrous membranes for wound dressing. *International Journal of Biological Macromolecules*. 2021, vol. 183, p. 68–78. DOI: https://doi.org/10.1016/j.ijbiomac.2021.04.021. ISSN 0141-8130. Available at: https://www.sciencedirect.com/science/article/pii/S0141813021007765.

[40] Basu, A. Ion-Crosslinked Nanocellulose Hydrogels for Advanced Wound Care Applications. In:. 2018. ISBN 978-91-513-0474-8.

[41] Britto, E. J., Nezwek, T. A. and Robins, M. *Wound Dressings*. StatPearls Publishing, Treasure Island (FL), 2020. Available at: http://europepmc.org/books/NBK470199.

[42] Adair, T. and Montani, J. *Angiogenesis*. Morgan & Claypool Life Sciences, 2011. Colloquium Series on Integrated Systems Physiology: from Molecule to Function to Disease Series. ISBN 9781615043309. Available at: https://books.google.cz/books?id=ykn66NeaPakC.

[43] Day, R. 6 - Functional requirements of wound repair biomaterials. In: Farrar, D., ed. *Advanced Wound Repair Therapies*. Woodhead Publishing, 2011, p. 155–173. Woodhead Publishing Series in Biomaterials. DOI: https://doi.org/10.1533/9780857093301.2.155. ISBN 978-1-84569-700-6. Available at: https://www.sciencedirect.com/science/article/pii/B978184569700650005X.

[44] Rippon, M., Ousey, K. and Cutting, K. Wound healing and hyper-hydration: a counterintuitive model. *Journal of Wound Care*. 2016, vol. 25, no. 2, p. 68–75. DOI: 10.12968/jowc.2016.25.2.68. PMID: 26878298. Available at: https://doi.org/10.12968/jowc.2016.25.2.68.

[45] Pastar, I., Stojadinovic, O., Yin, N., Ramirez, H., Nusbaum, A. et al. Epithelialization in Wound Healing: A Comprehensive Review. *Advances in wound care*. july 2014, vol. 3, p. 445–464. DOI: 10.1089/wound.2013.0473.

[46] Tan, S. and Dosan, R. Lessons From Epithelialization: The Reason Behind Moist Wound Environment. *The Open Dermatology Journal*. july 2019, vol. 13, p. 34–40. DOI: 10.2174/1874372201913010034.

[47] Le, A. D. and Brown, J. J. Chapter 2 - Wound Healing: Repair Biology and Wound and Scar Treatment. In: Bagheri, S. C., Bell, R. B. and Khan, H. A., ed. *Current Therapy In Oral and Maxillofacial Surgery*. Saint Louis: W.B. Saunders, 2012, p. 6–10. DOI: https://doi.org/10.1016/B978-1-4160-2527-6.00002-5. ISBN 978-1-4160-2527-6. Available at: https://www.sciencedirect.com/science/article/pii/B9781416025276000025.

[48] Williams, I. R. Fibroblasts. In: Delves, P. J., ed. *Encyclopedia of Immunology (Second Edition)*. Second Editionth ed. Oxford: Elsevier, 1998, p. 905–909. DOI: https://doi.org/10.1006/rwei.1999.0237. ISBN 978-0-12-226765-9. Available at: https://www.sciencedirect.com/science/article/pii/B0122267656002486.

[49] Pratt, J. and West, G., ed. 1 - Pressure therapy: history and rationale. In: Pratt, J. and West, G., ed. *Pressure Garments*. Butterworth-Heinemann, 1995, p. 1–21. DOI: https://doi.org/10.1016/B978-0-7506-2064-2.50006-4. ISBN 978-0-7506-2064-2. Available at: https://www.sciencedirect.com/science/article/pii/B9780750620642500064.

[50] Jones, K. Chapter 9 - Fibrotic Response to Biomaterials and all Associated Sequence of Fibrosis. In: Badylak, S. F., ed. *Host Response to Biomaterials*. Oxford: Academic Press, 2015, p. 189–237. DOI: https://doi.org/10.1016/B978-0-12-800196-7.00009-8. ISBN 978-0-12-800196-7. Available at: https://www.sciencedirect.com/science/article/pii/B9780128001967000098.

[51] Uzun, M. A review of wound management materials. *Journal of Textile Engineering & Fashion Technology*. january 2018, vol. 4. DOI: 10.15406/jteft.2018.04.00121.

[52] *Gelová permeační chromatografie (GPC)/Size Exclusion Chromatography(SEC)* [online]. Praha: Vysoká škola chemicko-technologická v Praze, 2018 [cit. 2021-05-10]. Available at: https://web.vscht.cz/~poustkaj/ISM%20PIGA%20Cz-13%20Gelov%C3%A1%20permea%C4%8Dn%C3%AD%20chromatografie_VH2018.pdf.

[53] *Viscosity of polymer solutions; Part I: Intrinsic viscosity of dilute solutions* [online]. Polymer Properties Database [cit. 2021-05-01]. Available at: https://polymerdatabase.com/polymer%20physics/Solution_Viscosity.html.

[54] Sebastiá, M. P. M. *Viscosity of polymers in solution* [online]. AIMPLAS, 2020 [cit. 2021-05-01]. Available at: https://www.aimplas.net/blog/viscosity-polymers-solution/.

[55] *Spinnability* [online]. The Free Dictionary [cit. 2021-05-01]. Available at: https://www.thefreedictionary.com/spinnability.

[56] *Stanovení objemového zlomku výztuže FRC a částicových kompozitů (TGA)* [online]. Brno: E-learning na VUT v Brně [cit. 2021-05-10]. Available at: https://moodle.vutbr.cz/pluginfile.php/220346/mod_resource/content/48.%20Stanoven%C3%AD%20objemov%C3%A9ho%20zlomku%20v%C3%BDztu%C5%BEe%20%C4%8D%C3%A1sticov%C3%BDch%20kompozit%C5%AF%20%28TGA%29%202018.pdf.

[57] Bálková, R. *STRUKTURA A VLAST. POLYMERNÍCH MATERIÁLŮ - Diferenční kompenzační kalorimetrie (DSC)* [online]. Brno: E-learning na VUT v

Brně [cit. 2021-05-10]. Available at:
https://moodle.vutbr.cz/pluginfile.php/112100/mod_resource/content/1/DSC.pdf.

[58] *Electron microscope* [online]. New World Encyclopedia: Research begins here [cit. 2021-04-29]. Available at:
http://www.newworldencyclopedia.org/entry/Electron_microscope.

[59] *Confocal Laser Scanning Microscope Olympus Lext OLS4100 (LEXT-OLS4100)* [online]. CEITEC, 2012 [cit. 2021-05-01]. Available at: https://www.ceitec.cz/confocal-laser-scanning-microscope-olympus-lext-ols4100/e1552.

[60] *Tahová zkouška polymeru (Sililab)* [online]. Brno: E-learning na VUT v Brně [cit. 2021-05-10]. Available at: https://moodle.vutbr.cz/mod/resource/view.php?id=90890.

[61] Rajendran, S. *Advanced Textiles for Wound Care*. Elsevier Science, 2009. Woodhead Publishing Series in Textiles. ISBN 9781845696306. Available at:
https://books.google.cz/books?id=M-6iAgAAQBAJ.

[62] TURK, E. LETTERS. *Chemical & Engineering News Archive*. 1998, vol. 76, no. 9, p. 6. DOI: 10.1021/cen-v076n009.p006. Available at:
https://doi.org/10.1021/cen-v076n009.p006.

List of Figures

List of Tables

List of Appendices

A SEM images from the optimization of spinnability of P3HB solutions

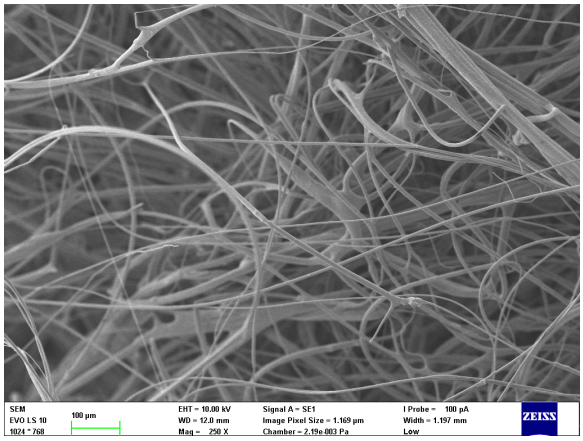

Figure A.1: SEM image of fibres prepared from 3 wt.% P3HB solution by rotational speed of 4,000 RPM

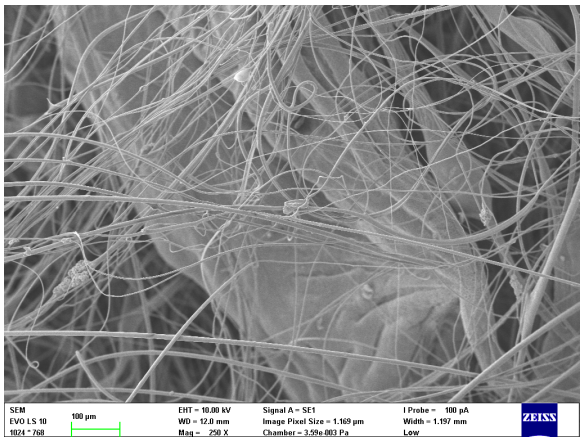

Figure A.2: SEM image of fibres prepared from 3 wt.% P3HB solution by rotational speed of 5,000 RPM

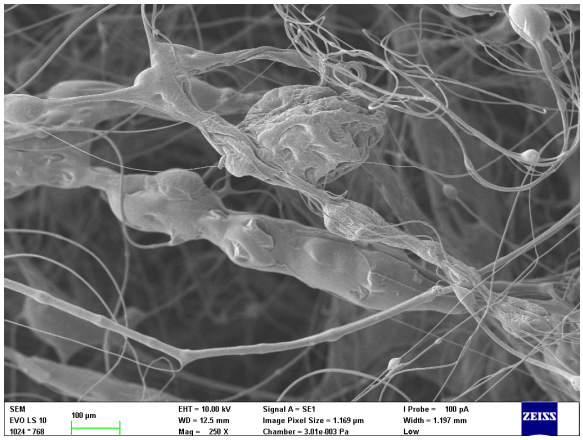

Figure A.3: SEM image of fibres prepared from 3 wt.% P3HB solution by rotational speed of 8,000 RPM

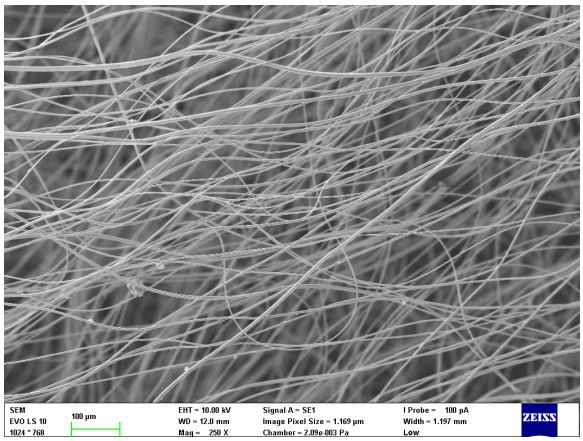

Figure A.4: SEM image of fibres prepared from 5 wt.% P3HB solution by rotational speed of 4,000 RPM

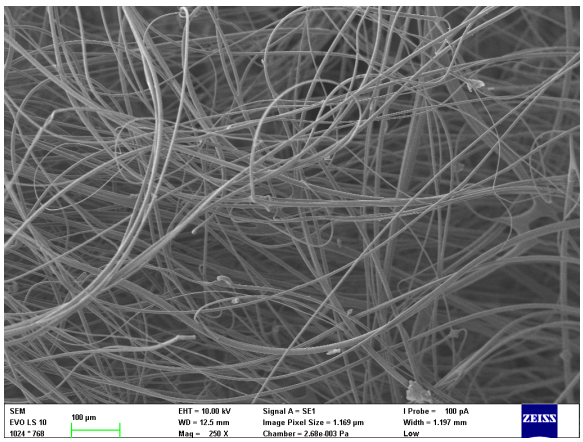

Figure A.5: SEM image of fibres prepared from 5 wt.% P3HB solution by rotational speed of 5,000 RPM

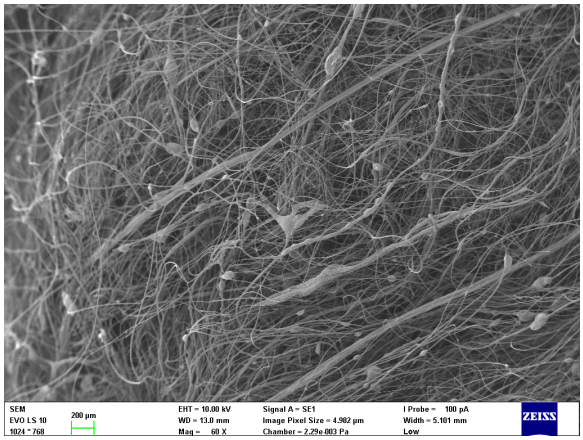

Figure A.6: SEM image of fibres prepared from 5 wt.% P3HB solution by rotational speed of 8,000 RPM

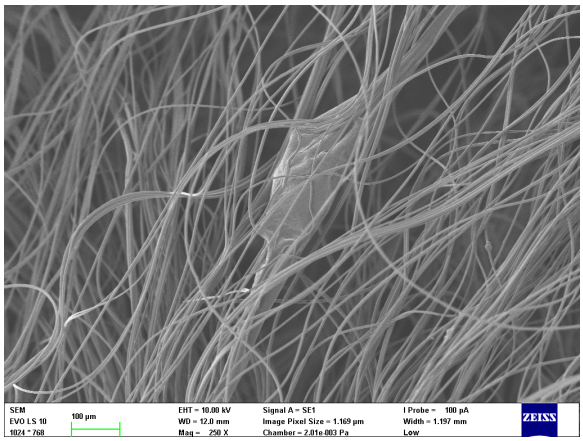

Figure A.7: SEM image of fibres prepared from 7 wt.% P3HB solution by rotational speed of 4,000 RPM

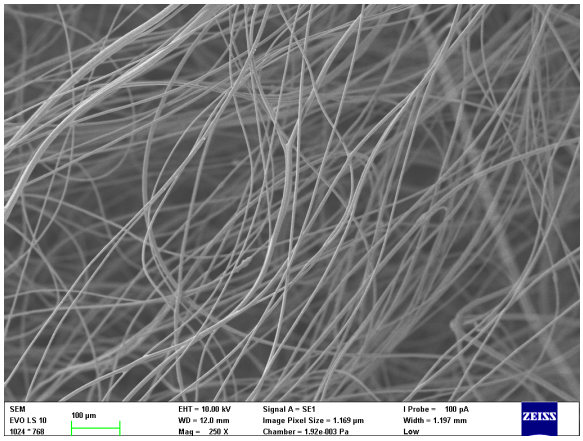

Figure A.8: SEM image of fibres prepared from 7 wt.% P3HB solution by rotational speed of 5,000 RPM

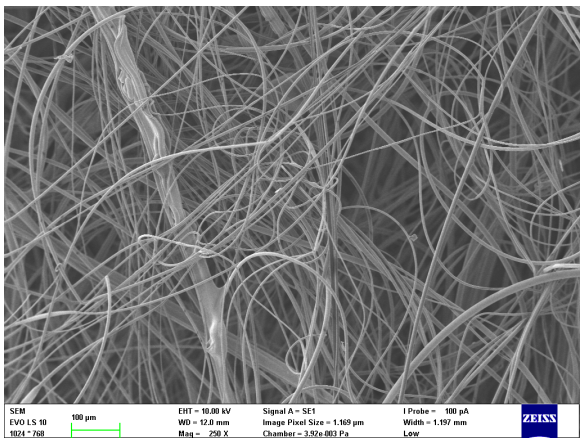

Figure A.9: SEM image of fibres prepared from 7 wt.% P3HB solution by rotational speed of 8,000 RPM

B Tensile test results

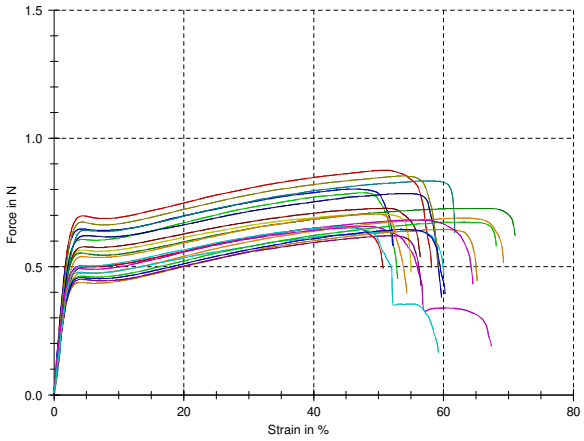

Figure B.1: Force dependence on the strain of planar sample P3HB

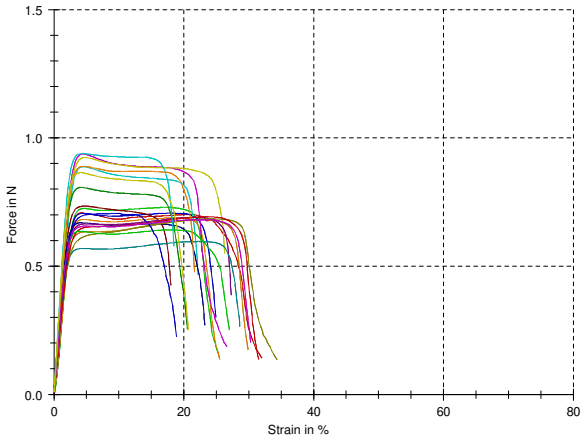

Figure B.2: Force dependence on the strain of planar sample P3HB:PLA (70:30)

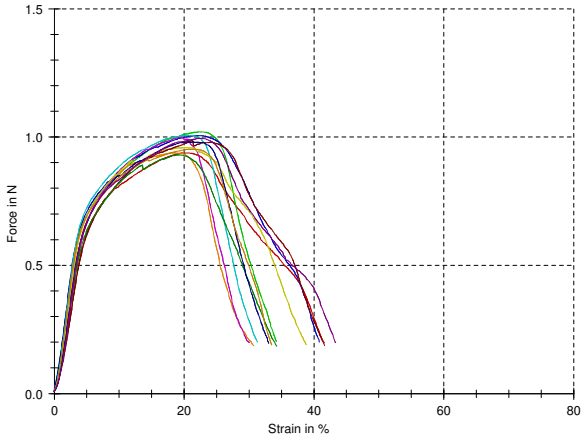

Figure B.3: Force dependence on the strain of planar sample PLA

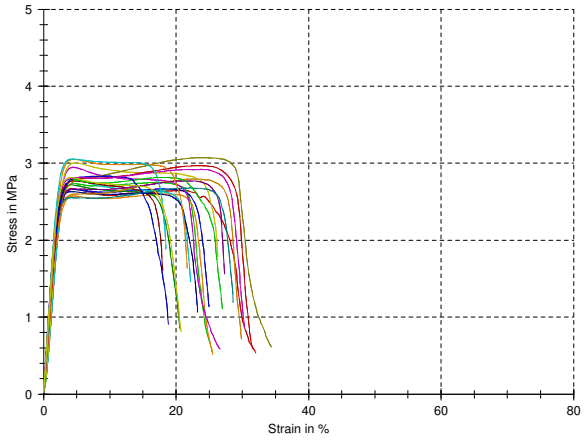

Figure B.4: Force dependence on the strain of planar sample P3HB:PCL (70:30)

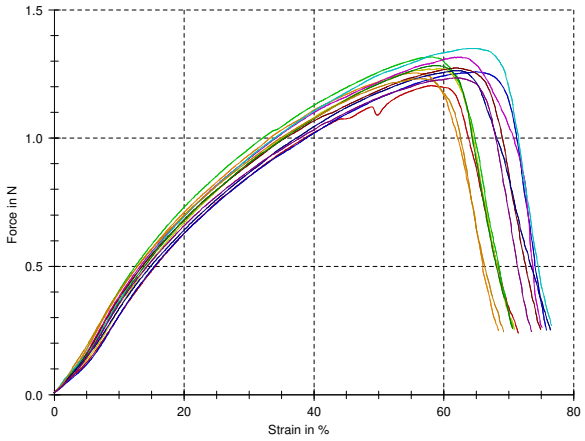

Figure B.5: Force dependence on the strain of planar sample PCL

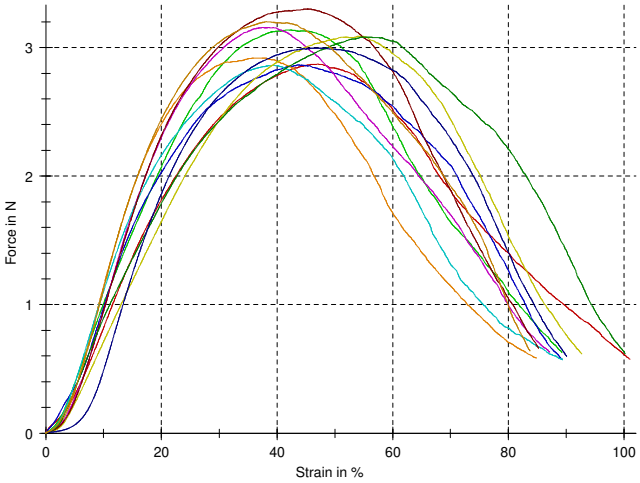

Figure B.6: Force dependence on the strain of cotton-like reference sample P3HB

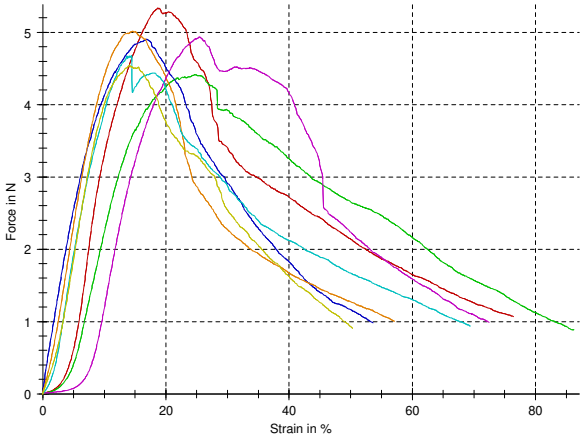

Figure B.7: Force dependence on the strain of cotton-like sample P3HB with the addition of 5 wt.% Syncroflex plasticiser

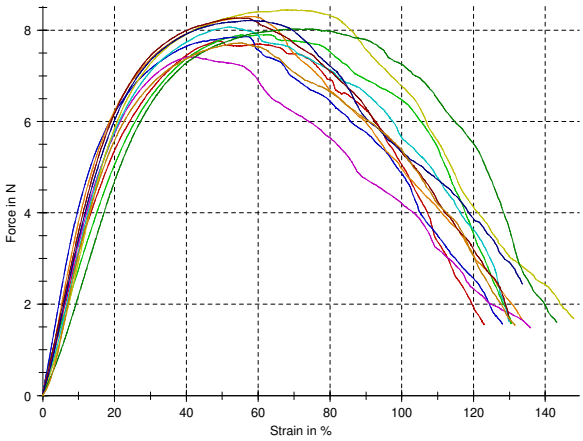

Figure B.8: Force dependence on the strain of cotton-like sample P3HB with the addition of 15 wt.% Syncroflex plasticiser

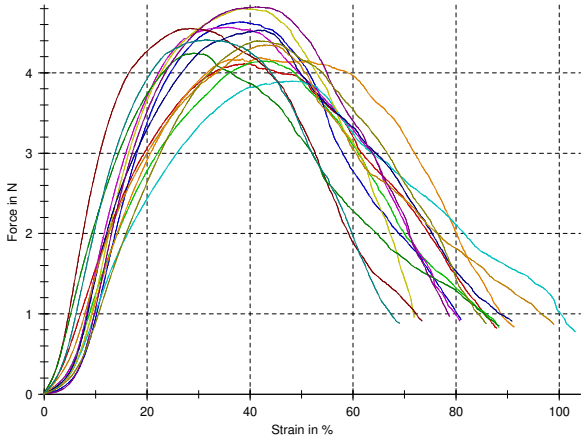

Figure B.9: Force dependence on the strain of cotton-like sample P3HB with the addition of 5 wt.% A4 plasticiser

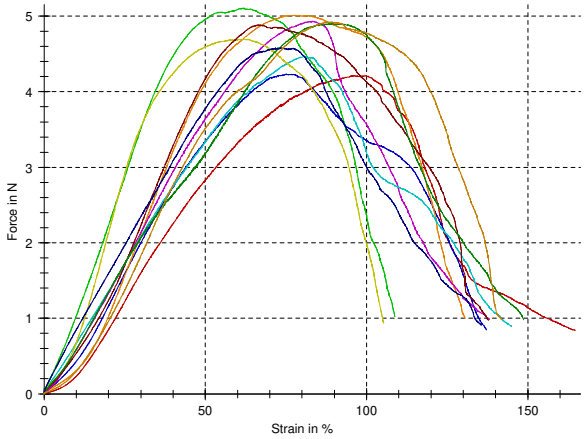

Figure B.10: Force dependence on the strain of cotton-like sample P3HB with the addition of 10 wt.% A4 plasticiser

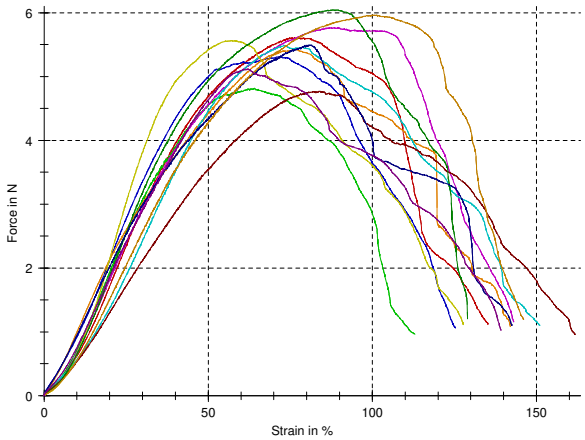

Figure B.11: Force dependence on the strain of cotton-like sample P3HB with the addition of 15 wt.% A4 plasticiser

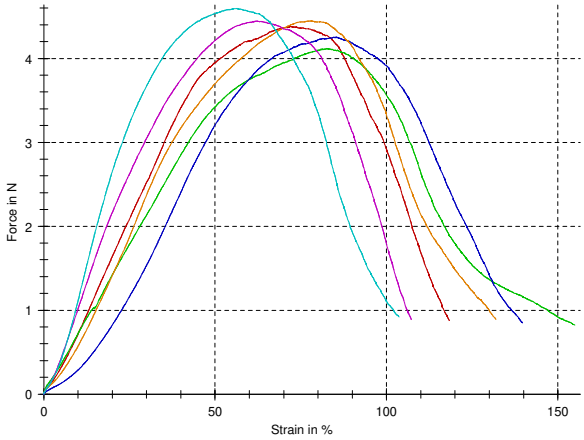

Figure B.12: Force dependence on the strain of cotton-like sample P3HB with the addition of 5 wt.% EMERY MC 2192 plasticiser

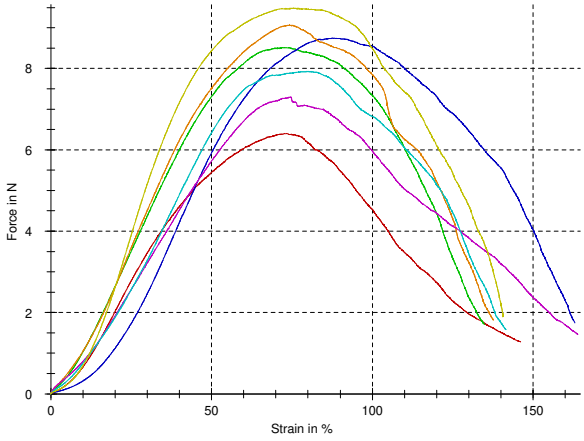

Figure B.13: Force dependence on the strain of cotton-like sample P3HB with the addition of 15 wt.% EMERY MC 2192 plasticiser

C Decrease in molecular weight of P3HB over time

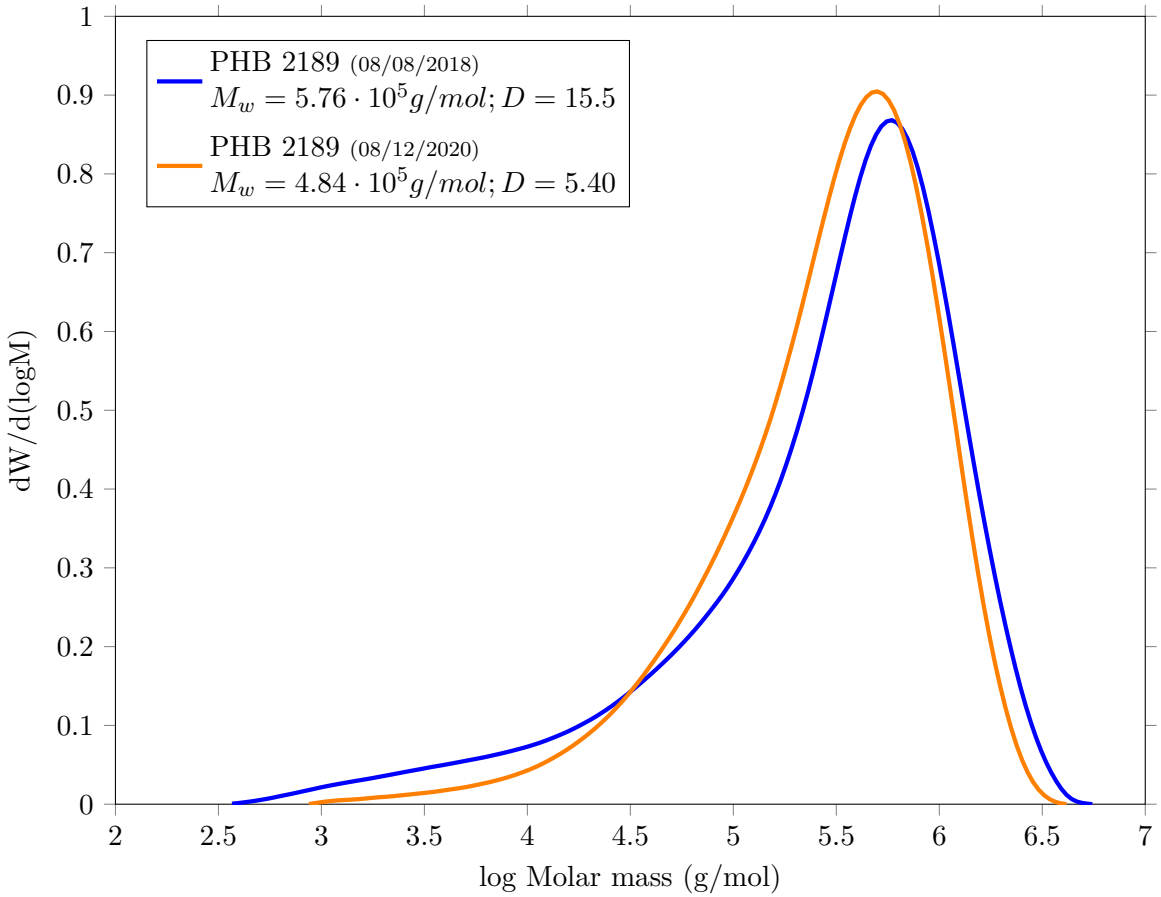

Figure C.1: The decrease in molecular weight of P3HB 2189 powder over two years